Technical Report

TR-02-04

Vertical seismic profiling and integration with reflection seismic studies at Laxemar, 2000

Christopher Juhlin, Björn Bergman
University of Uppsala

Calin Cosma, Jukka Keskinen, Nicoleta Enescu
Vibrometric Oy

February 2002

Svensk Kärnbränslehantering AB
Swedish Nuclear Fuel
and Waste Management Co
Box 5864
SE-102 40 Stockholm Sweden
Tel 08-459 84 00
+46 8 459 84 00
Fax 08-661 57 19
+46 8 661 57 19

Vertical seismic profiling and integration with reflection seismic studies at Laxemar, 2000

Christopher Juhlin, Björn Bergman
University of Uppsala

Calin Cosma, Jukka Keskinen, Nicoleta Enescu
Vibrometric Oy

February 2002

Keywords: VSP, seismics, reflectors, SIST source, sonic

This report concerns a study which was conducted for SKB. The conclusions and viewpoints presented in the report are those of the author(s) and do not necessarily coincide with those of the client.

Abstract

Vertical seismic profile (VSP) data were acquired in October 2000 in the 1700 m deep KLX02 borehole, near Laxemar in southeastern Sweden. Five primary source points were used, one close to the wellhead and the other four offset by about 200−400 m. Only at the wellhead was an explosive source used. A swept impact seismic source (SIST) was also used at all five source points. Three groups of reflections are observed. A sub−horizontal set that is interpreted to originate from greenstone lenses; a moderately dipping one consisting of two sub−groups, one dipping to the NNW and the other to the SSE; and a steeply dipping one that strikes at 50−70° and dips at 70−80° to the SE. The sub−horizontal group and the NNW moderately dipping sub−group are also observed on the surface seismic. Comparison of the explosive source VSP with that from the coincident SIST VSP shows comparable amounts of energy were recorded, with the SIST source having a more more consistent waveform, but at lower frequency levels. It is recommended that a SIST source be used in future VSP studies with at least 10 source points to ensure that reflections can be correlated from source point to source point. Use of a source array, rather than a single point, would further enhance the VSP method.

Sammanfattning

Borrhålsseismisk (VSP) utfördes under oktober 2000 i det 1700 m djupa KLX02 borrhålet, nära Laxemar i sydöstra Sverige. Fem primära källpunkter användes, en nära borrhålet och de andra fyra ca 200−400 m bort. Dynamit användes som störkälla endast vid borrhålet. En "swept impact seismic source" (SIST) användes vid alla fem källpunkterna. Observerade seismiska reflektioner kan indelas i tre grupper; en sub−horisontal grupp som härstammar från grönstenslinser; en måttligt stupande grupp som kan indelas i två sub−grupper, en som stupar NNV och den andra SSO; och en brant stupande grupp som stryker 50−70° och stupar 70−80° mot SO. Den sub−horisontella gruppen och den NNV stupande sub−gruppen observeras också på ytseismiken. Energinivåer från dynamit och SIST källorna är ungefär detsamma, SIST källan har en mer jämn vågform, men med lägre frekvensinnehåll. Det rekommenderas att SIST källan används i framtida VSP undersökningar med minst 10 källpunkter för att försäkra att reflektioner kan korreleras från den ena källpunkten till den andra. Användande av en källarray, istället för en enstaka punkt, skulle ytterligare förbättra VSP metoden.

Summary

Vertical seismic profile (VSP) data were acquired in October 2000 in the 1700 m deep KLX02 borehole, near Laxemar in southeastern Sweden. The objectives of the VSP were to image reflectors in the borehole for correlation with surface seismic and borehole data, study the signal penetration of explosive versus mechanical sources and determine the seismic velocity as a function of depth. Five principal source points were used, one located close to the KLX02 wellhead and 4 others that were offset by about 200 m to 400 m. An explosive source was only used at the wellhead and consisted of 15 grams of dynamite in 90 cm deep shot holes in bedrock. A swept impact seismic source (SIST) was also used at the wellhead, as well as at the other four offset source points. The primary SIST source consisted of a computer controlled mechanical hammer mounted on a tractor. By activating the hammer over a 15 second sweep length, the total energy transferred to the ground is on the same order as that produced by the dynamite. The recorded data are then processed to generate seismic records that are equivalent to a single impact source.

A smaller handheld SIST source was also tested at the wellhead. Tests of both the tractor mounted source and dynamite were made at a location offset somewhat from the wellhead at a site containing loose sediments at the surface. Full waveform sonic, resistivity and gamma logs were also acquired in conjunction the VSP survey.

A comparison between the explosive and large SIST source shows that comparable energy levels are produced by the two methods. The SIST source appears to be more stable in terms of the energy level, although the frequency content of data are somewhat lower. However, its most significant advantage is the low cost of preparation of the source points and the speed of the acquisition.

Numerous reflections are observed on the VSP, as is the case on the surface seismic, implying a complex structure in the vicinity of the KLX02 borehole. Three groups of reflections are observed. A sub−horizontal set that is interpreted to originate from greenstone lenses; a moderately dipping one consisting of two sub−groups, one dipping to the NNW and the other to the SSE; and a steeply dipping one that strikes at 50−70° and dips at 70−80° to the SE. Reflections from the two latter groups probably originate from fracture zones. The last group being responsible for the highly fractured zone between 1550 m and 1700 m. Reflections from the first sub−horizontal group and the NNW dipping sub−group are also observed on the surface seismic with the same general strike and dips. However, the estimated dips on the surface seismic are consistently lower. This may be explained by the VSP imaging the local reflector dip, while the surface seismic images the more larger scale regional dip. Dips and depth estimates to reflectors are generally known to an accuracy of better than ±5% on both surface seismic and VSP data if its strike is known and it is planar.

A special high resolution VSP survey was run in the cased part of the hole down to 200 m to image a clear 45° N dipping reflector on the surface seismic that intersects the borehole at the bottom of the casing at 200 m depth. This reflector generates PP and PS reflections and misinterpretation of the data can easily be done if the PS conversion is not taken into account.

Table of Contents

1. Introduction

SKB is currently carrying out studies to determine which seismic techniques, and how, they will be used for investigations prior to and during the building of a high−level nuclear waste repository. Active seismic methods included in these studies are refraction seismics, reflection seismics, and vertical seismic profiling (VSP). The main goal of the active seismic methods is to locate fracture zones in the crystalline bedrock. Plans are to use longer reflection seismic profiles (3−4 km) in the initial stages of the site investigations. The target depth for these seismic profiles is 100−1500 m. After acquiring and processing these profiles, boreholes will be drilled and VSP surveys will be performed. If necessary, 3D surface seismic surveys will be acquired. VSP and surface seismics are to a large extent complementary. However, the results of the two techniques overlap partially, which allows the preliminary interpretations of the two data sets to be verified and permits the planning for more detailed seismic studies.

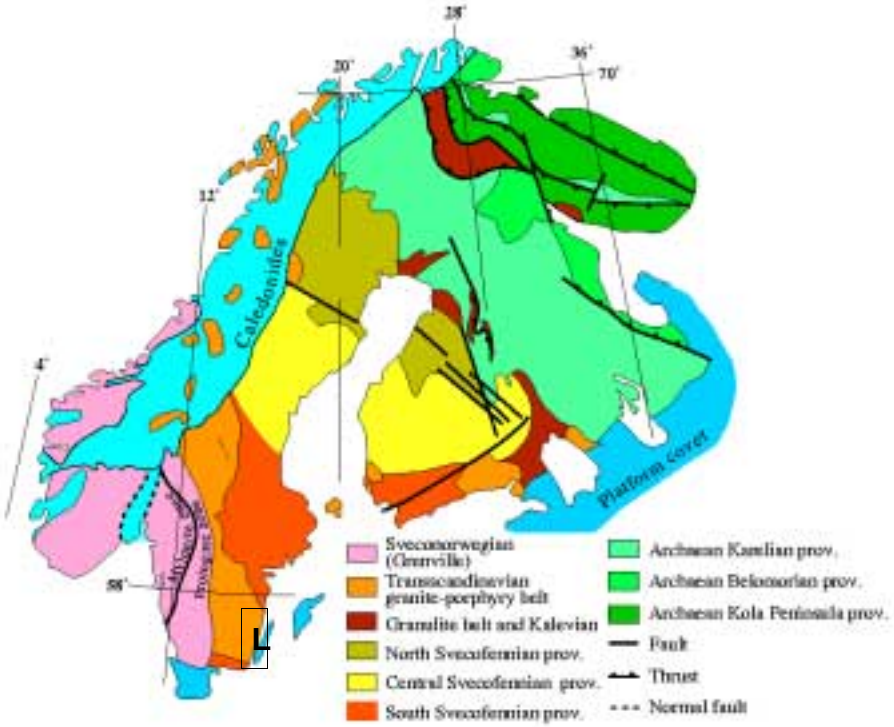

Figure 1−1*. General geology of the Baltic Shield and location of the Laxemar (L in figure) area (map after Weihed, 1992)*

After a series of tests of the seismic reflection method over SKB study sites (Cosma et al., 1994, Juhlin, 1995; Juhlin and Palm, 1999; Bergman et al., 2001; Juhlin et al., 2001) a method has been developed for acquiring good quality high resolution reflection seismic data over crystalline rock along 2D profiles at a relatively low cost (Juhlin et al., 2001). A full scale test of the reflection seismic method at Laxemar in southeastern Sweden, near Oskarshamn, (Figure 1−1) was carried out in 1999 consisting of two crossing profiles, a 2 km long SW−NE running one and a 2.5 km long SE−NW running one, both imaging numerous reflectors (Bergman et al., 2001). Some structural control on the 3D orientation of reflectors is obtained at the crossing point, the location of the c. 1700 m deep KLX02 borehole (Figure 1−2). In order to obtain improved structural control and verify the preliminary interpretation of the surface seismic data, VSP was carried out in the KLX02 borehole in October 2000.

VSP data acquisition was carried out by Vibrometric Oy, as was the wireline log acquisition. Surveying of shot points was done by Uppsala University. Processing and interpretation has been carried out jointly by Vibrometric Oy and Uppsala University.

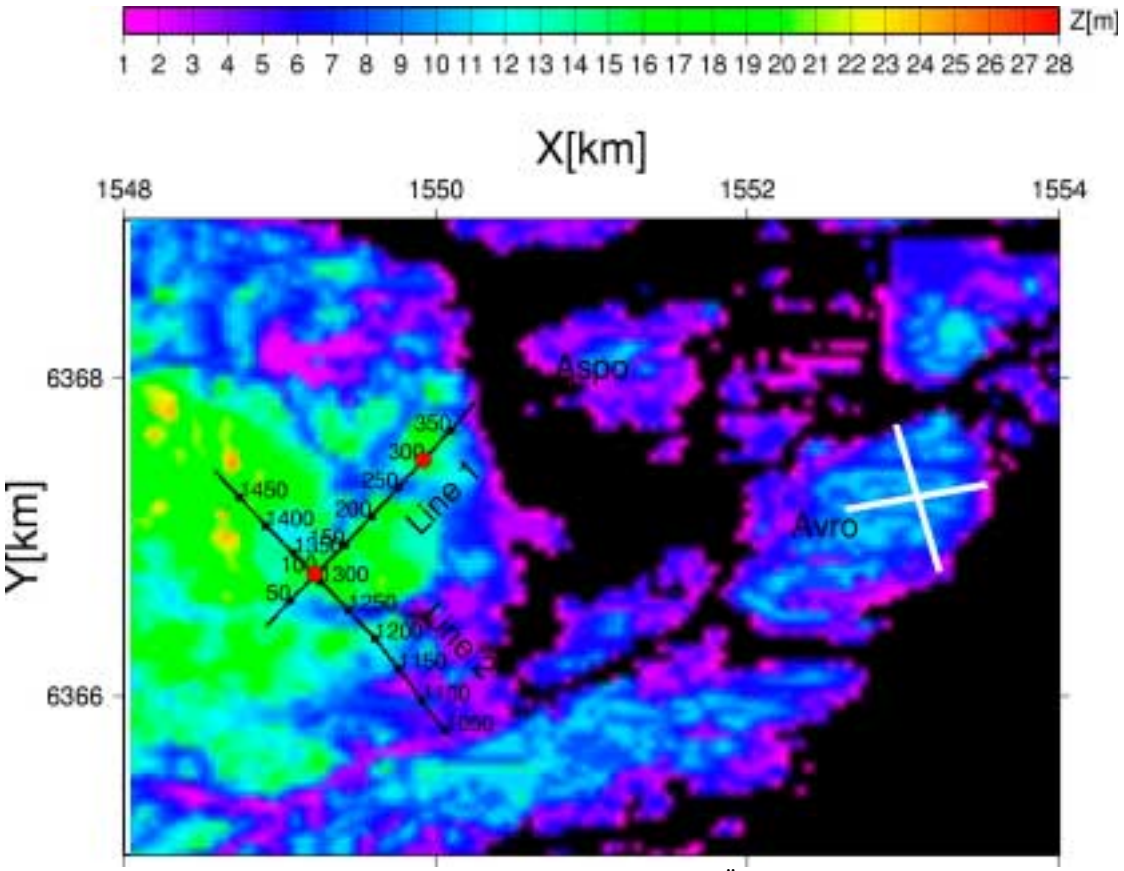

Figure 1−2*. Location of the Laxemar (Bergman et al., 2001) and Ävrö (Juhlin and Palm, 1999) seismic experiments and the KLX01 and KLX02 deep boreholes (red dots). Color bar refers to elevation of ground surface.*

2. VSP method

One of the main purposes of VSP is to determine where seismic reflectors intersect the borehole (Hardage, 2000). Borehole data can then be correlated with these intersection points to determine the origin of the reflections. In addition, if surface seismic data with some 3D control are available, the VSP can provide a quantitative link between the borehole data and the surface seismic. Figure 2−1 depicts a possible acquisition geometry with a 45° dipping reflector and source point offset downdip from the wellhead of the borehole. The reflector has physical properties that may be expected of a fracture zone, 10 m thick, and intersects the borehole at about 650 m depth. The main event on the synthetic seismogram is the downgoing wave (rays not shown) propagating directly from the source to the receiver in the borehole. This wave is observed at all depths in the borehole. The P−wave reflection (solid rays in Figure 2−1) is much weaker than the direct wave and is not observed below 650 m. Also present is the much weaker P−wave to S−wave converted reflection (PS wave) arriving later than the P−wave reflection (PP wave). The PS wave is relatively weak for the acquisition geometry in Figure 2−1, but can be considerably stronger for other acquisition geometries. This is the case in Figure 2−2 where the source point is located updip from the wellhead and the incidence angles are greater. In this case, the PS reflection is stronger than the PP reflection with the PP amplitude becoming very weak where the reflector intersects the borehole. In cases such as this the PS reflection may easily be mistaken for a PP reflection and the orientation of the reflector misinterpreted. It is only when incident P−waves impinge on a reflector at right angles that no PS waves are reflected. Figure 2−3 shows the same geometry as Figure 2−1, but with a much more dense receiver configuration, similar to what would be used in real acquisition.

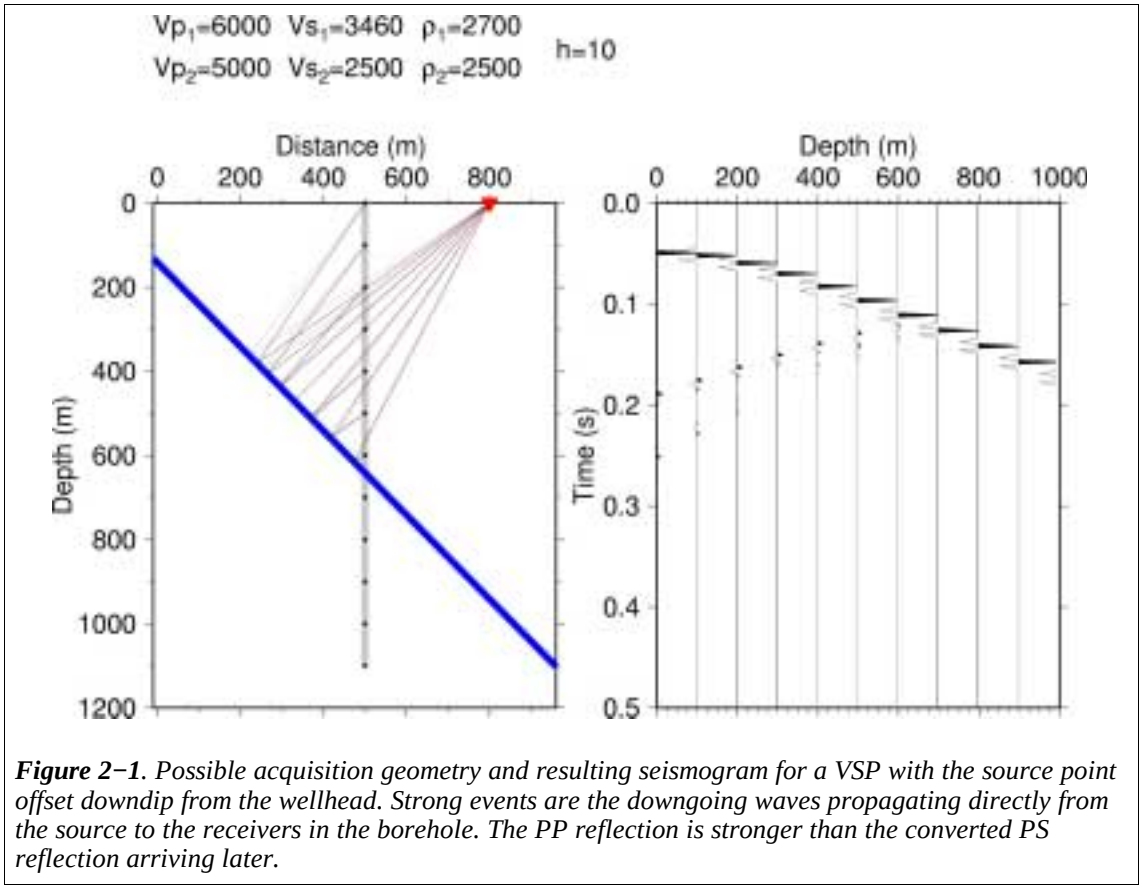

Figure 2−1*. Possible acquisition geometry and resulting seismogram for a VSP with the source point offset downdip from the wellhead. Strong events are the downgoing waves propagating directly from the source to the receivers in the borehole. The PP reflection is stronger than the converted PS reflection arriving later.*

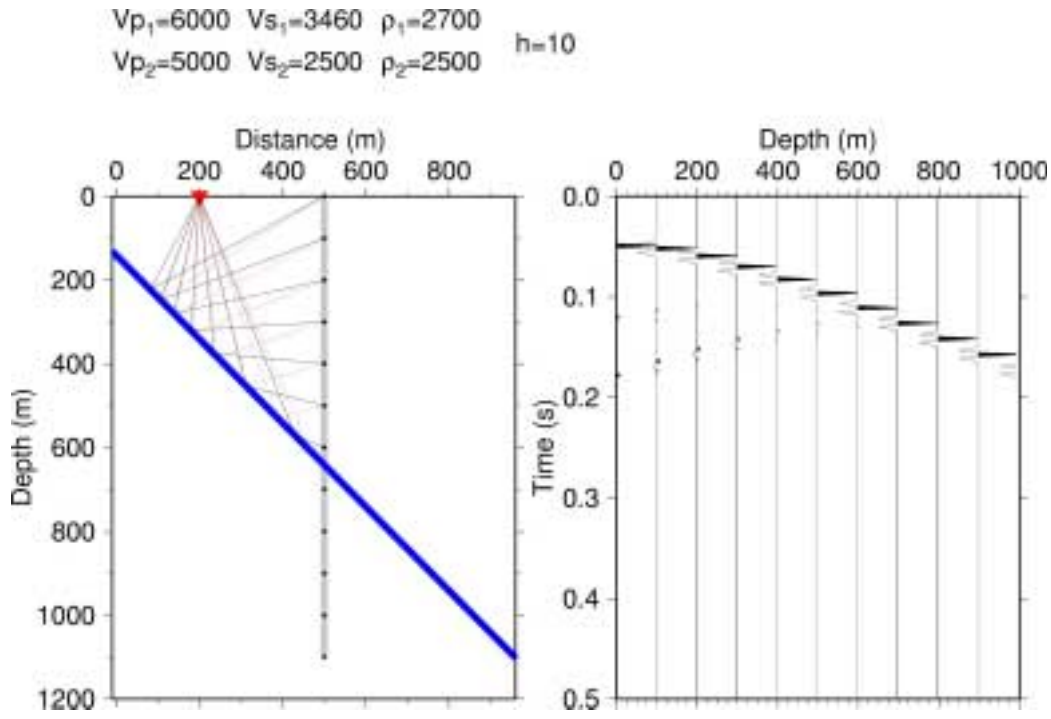

Figure 2−2*. Possible acquisition geometry and resulting seismogram for a VSP with the source point offset updip from the wellhead. Here the converted PS reflection is the stronger event while the PP reflection is weaker and almost not visible close to the borehole.*

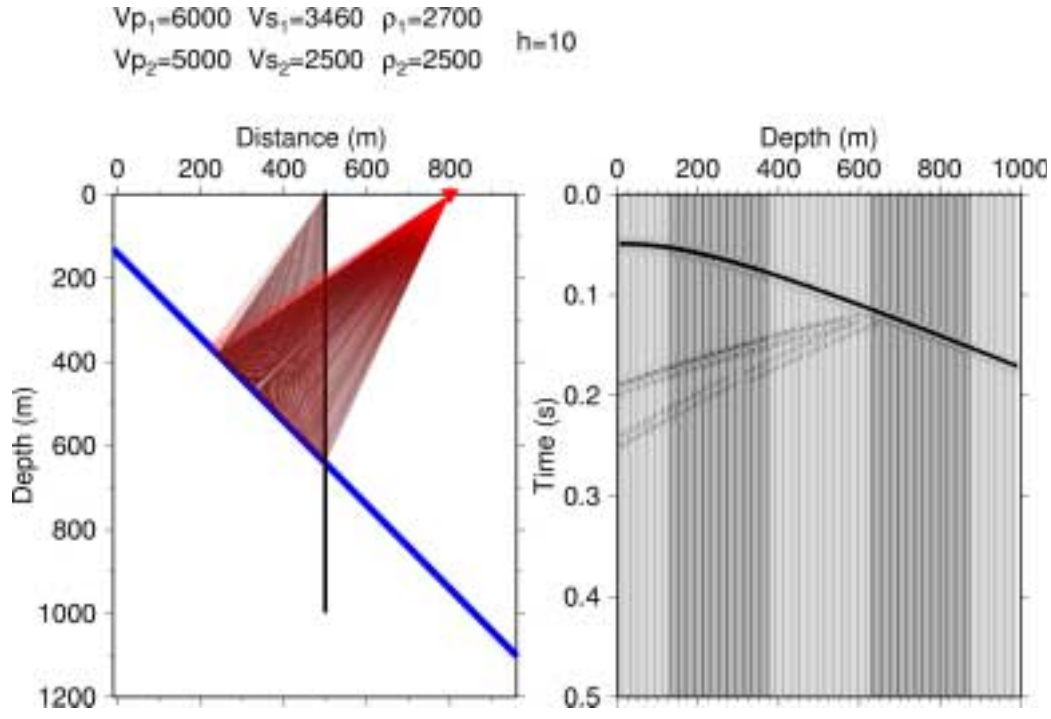

Figure 2−3*. A densely spaced synthetic VSP highlighting the differences in the amplitudes and traveltimes for the reflected P and converted PS reflections.*

3. Previous studies at Laxemar

3.1. Geology

The bedrock in the survey area is part of the Småland mega−block, a crustal segment stable since late Precambrian times (Milnes et al., 1999). The Småland mega−block is part of the Trans−Scandinavian Igneous Belt (TIB) (Figure 1−1)which intruded c. 1.8 Ga ago (Gorbatschev and Bogdanova, 1993). The lithology in the survey area is dominated by porphyritic fine− to medium−grained red to reddish granites, granodiorites and quartz monzodiorites. Early ductile deformation was followed by intermediate semi−ductile and younger brittle deformation (Talbot, 1990). A ductile deformation zone crosses Line 1 at its southern end. E−W and NE−SW fracture/fault zones are present on different scales and appear to have reactivated older semi−ductile shear zones. Other major structures are younger N−S, NNW−SSE to NW−SE trending zones that are believed to represent vertical to sub−vertical fracture zones. About half of the surface area shows exposed bedrock while the remaining part is covered by peat and glacial till. The thickness of the soil cover varies from 0 m up to about 20 m.

3.2. Laxemar reflection seismic experiment

The prime objective of this experiment was to perform a full−scale test of a method using slim shot holes and small explosive sources for mapping the upper kilometers of the crystalline crust. The shot holes were 12−20 mm in diameter and the charges varied in the range 15−75 grams. Two deep boreholes were drilled earlier in the survey area, depths of 1700 m (KLX02) and 1078 m (KLX01). A secondary objective of the experiment was to map fracture zones three dimensionally that are present in the area and that intersect the boreholes. The upper 1−2 km of crystalline bedrock can be mapped with high−resolution reflection seismics using small explosive sources in areas such as Laxemar where the cover of loose sediments is thin or absent. After testing and development, a good compromise between charge size and shot hole dimension has been determined to be 15 grams in 90 cm deep 12 mm diameter shot holes in bedrock outcrops and 75 grams in 150 cm deep 20 mm diameter (cased to 16 mm) shot holes in loose sediments.

Two crossing profiles were acquired over the 1700 m deep KLX02 borehole, a 2 km long NE−SW running one (Line 1) and a 2.5 km long NW−SE running one (Line 2). Where the two profiles cross, it is possible to orient several dipping reflectors and determine where they intersect the KLX02 borehole (Figure 3−1). Based on correlation with borehole data and surface geology, many of these reflectors appear to be related to fracture zones, some of which have high hydraulic conductivity. However, the presence of greenstones, that have a significant impedance contrast to the surrounding granite, in the borehole may also enhance the reflectivity. Some reflections present only on single lines may originate entirely from greenstone bodies. Regardless of the source of the reflections it is important for nuclear waste disposal site studies and other deeper underground construction applications to know where these reflectors will be encountered at depth.

Table 3−1. Orientation of reflectors as determined from the surface seismic and shown in Figure 3−2. Distance refers to distance from the KLX02 wellhead to the closest point on the reflector at the surface. Depth refers to depth below the surface which the reflector is located in the KLX02 borehole. Strike is measured clockwise from north.

Reflector	*Strike*	*Dip*	*Distance (m)*	*Depth (m)*	*Velocity (m/s)*
A	268	43	190	195	5600
Ba	180	3		610	5800
B	0	3		780	5800
Bb	0	3		950	5800
C	90	49	1530	1610	5800
D	253	35	840	650	5800
E	90	8		1275	5800
G	253	35	1170	910	5800

Where the two lines cross it is possible to determine the 3D orientation of certain reflectors (Table 3−1). Reflections from these interfaces have been modeled and are indicated on the two surface seismic lines (Figure 3−2). The strikes and dips of these reflectors are somewhat different than those presented in Bergman et al. (2001) after a more thorough analyses of the surface seismic data. There are numerous sub−horizontal reflections below Ba continuing down to about Bb. These two reflections have been chosen to mark the limits of this reflective zone with reflection B being, perhaps, the most distinct. These sub−horizontal reflections are less continuous on Line 2 than on Line 1 with some indications of them being offset, suggesting the presence of sub−vertical faulting perpendicular to Line 2.

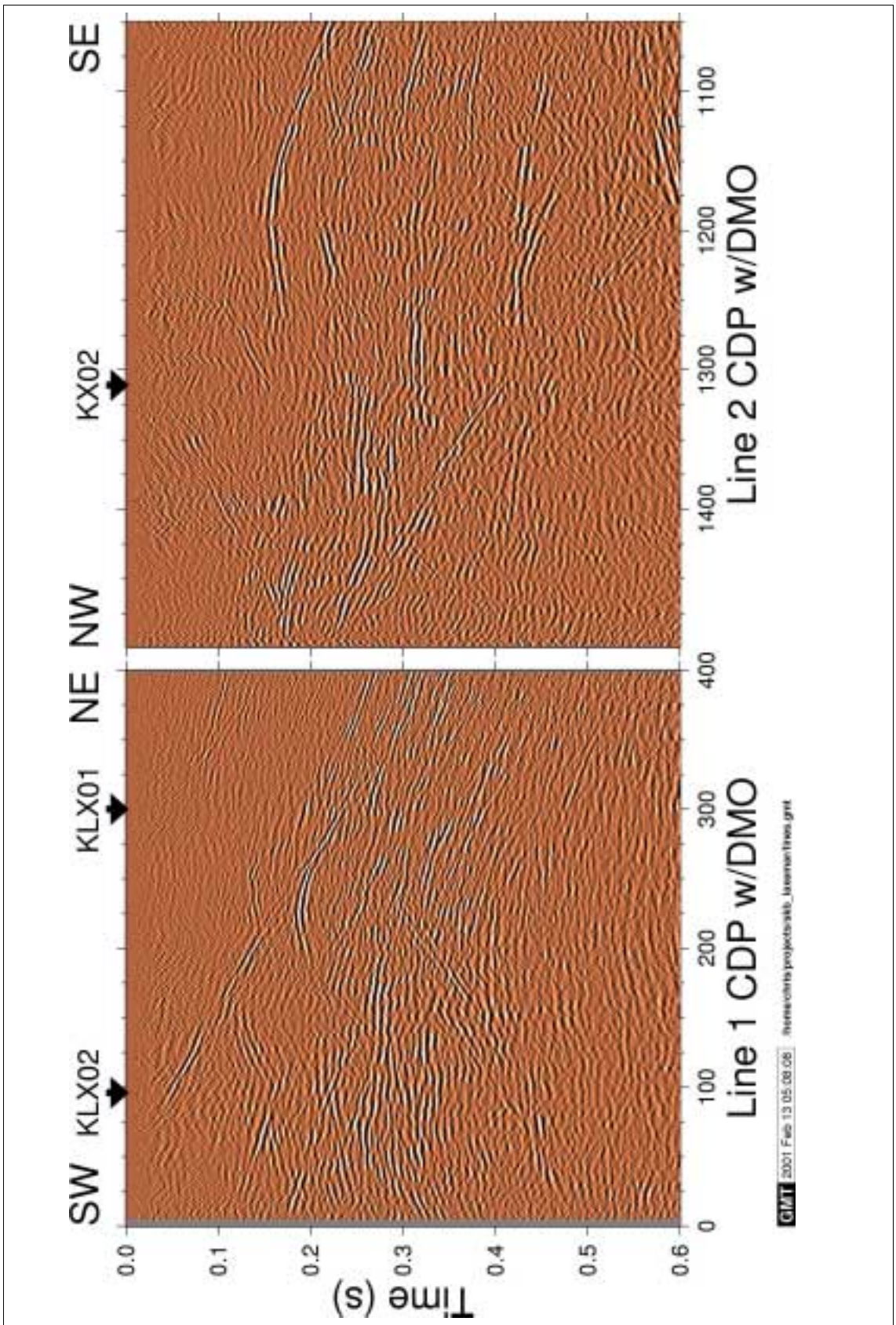

Figure 3−1*. Stacked seismic sections of Lines 1 and 2.*

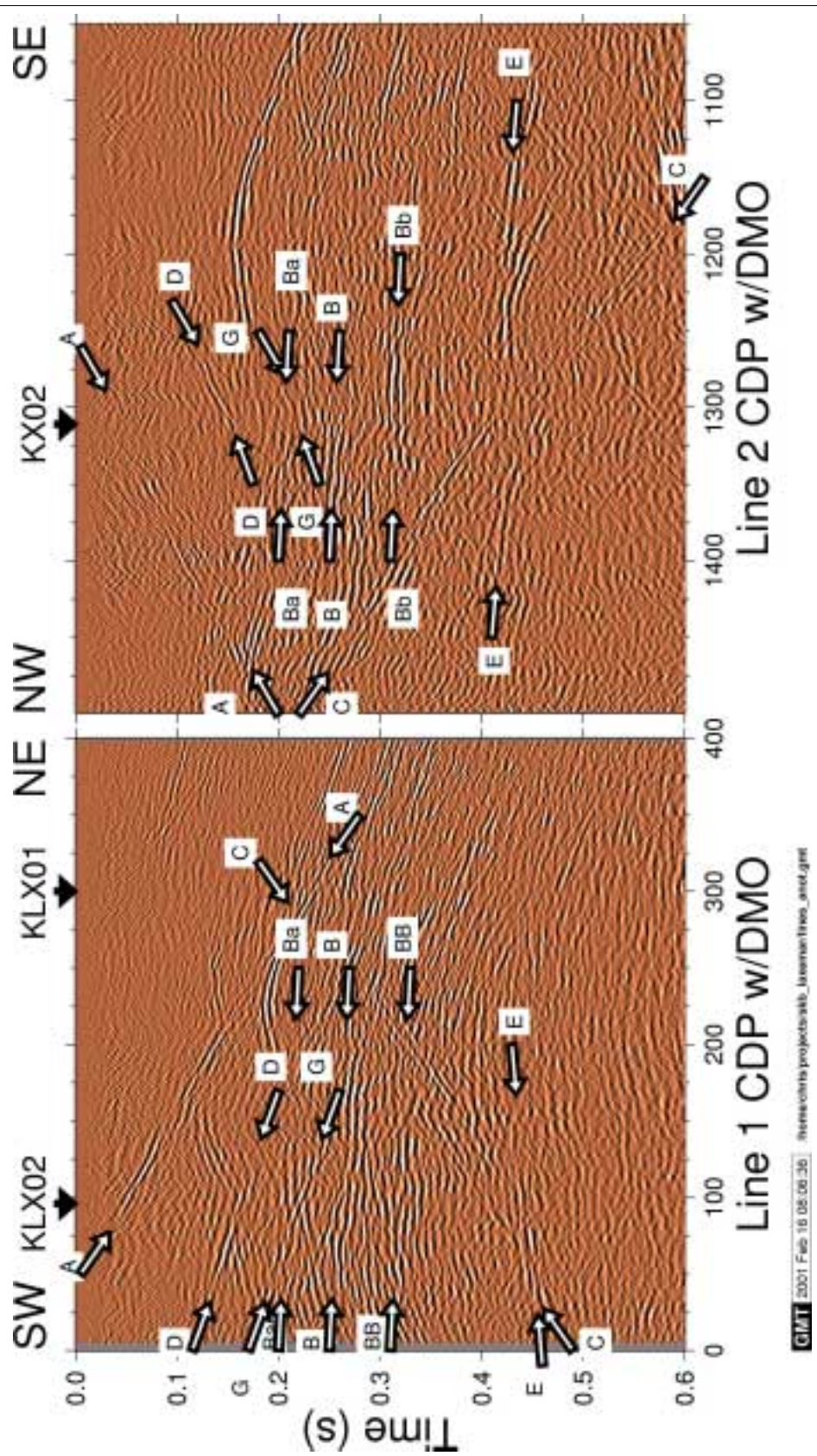

Figure 3−2*. Stacked seismic sections of Lines 1 and 2 with modeled interfaces from Table 3−1. See text for a discussion of the marked reflections.*

3.3. Borehole data

An extensive number of measurements have been carried out in the KLX01 and KLX02 boreholes, including coring and hydraulic tests (Ekman, 2001), as well as wireline logging. Several sections of the boreholes are hydraulically conductive indicating fractures or fracture zones. No core was taken from the upper 200 m of the KLX02 borehole. Below this depth, zones of significantly increased fracturing are observed at the following depths, 210−280 m, 390 m, 470 m, 780−1080 m, 1120 m, 1200 m and 1550−1700 m (Ekman, 2001). Lower sonic velocities characterize all of these, except for the one at 1200 m, which is associated with a greenstone interval. The lowermost one was not logged and, therefore, its sonic velocity is unknown.

The KLX02 borehole is not completely vertical, it is inclined at about 5° from vertical to the north resulting in an offset from the wellhead of about 160 m at the bottom of the borehole (Figure 3−3). This deviation from vertical adds additional complication to interpreting the surface seismic since 3D control is only obtained exactly where the lines cross. The reflectivity can change dramatically over 100 m as evidenced by the surface seismic data in Figure 3−1.

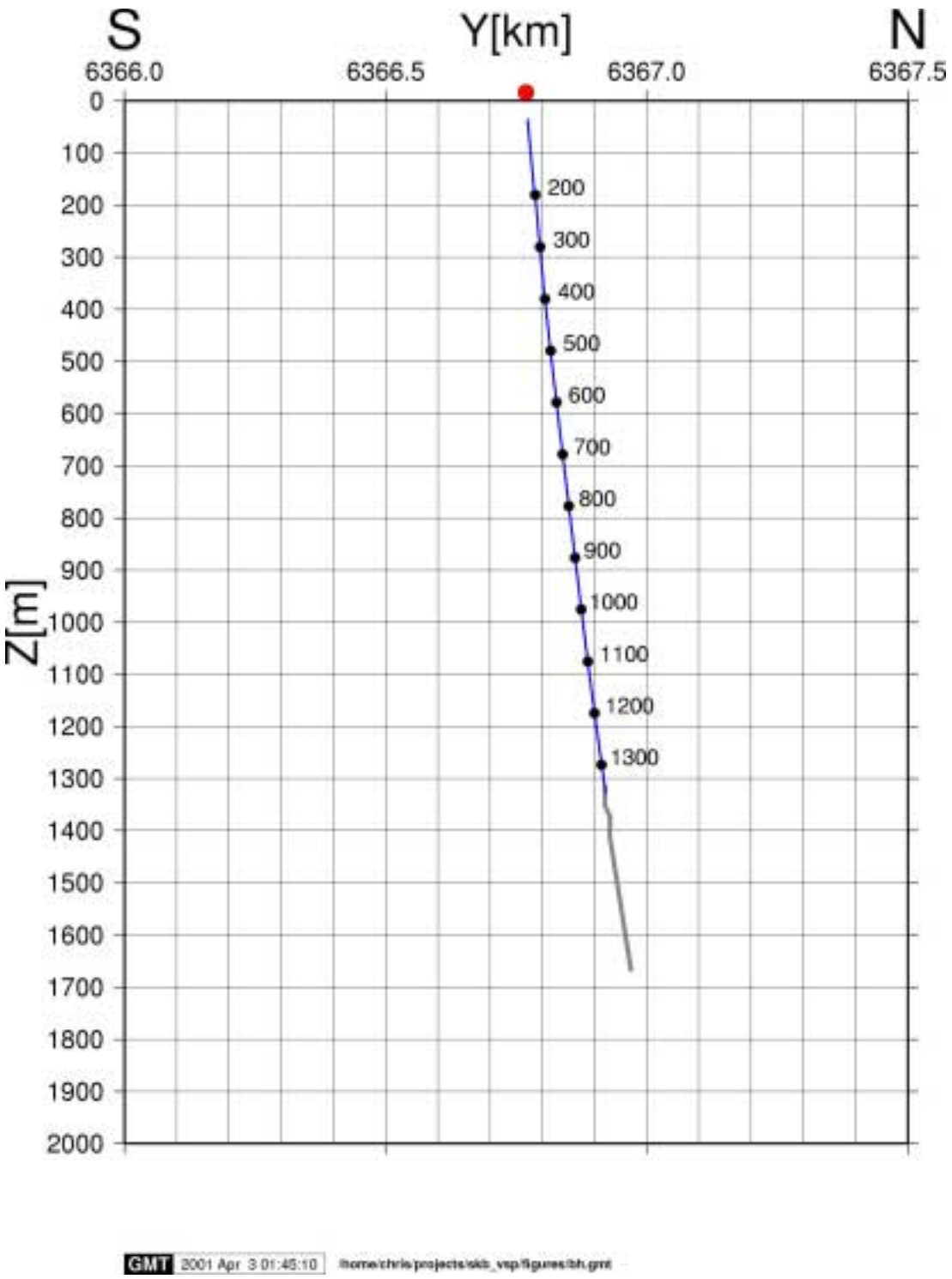

Figure 3−3*. NS−vertical plane view of the geometry of the KLX02 borehole. Every 100 m of measured depth along the VSP survey are marked. The borehole extends to a measured depth of about 1700 m.*

4. Wireline logs

The following wireline logs were run in the borehole prior to VSP acquisition:

- Full−waveform sonic (Vp and Vs)
- Natural gamma
- Resistivity

The data were acquired from 200 m to 1000 m, the limit of the logging cable, using equipment from Laval University, Canada (see Appendix A−1 for details).

Results from the logging are shown in Figure 4−1.

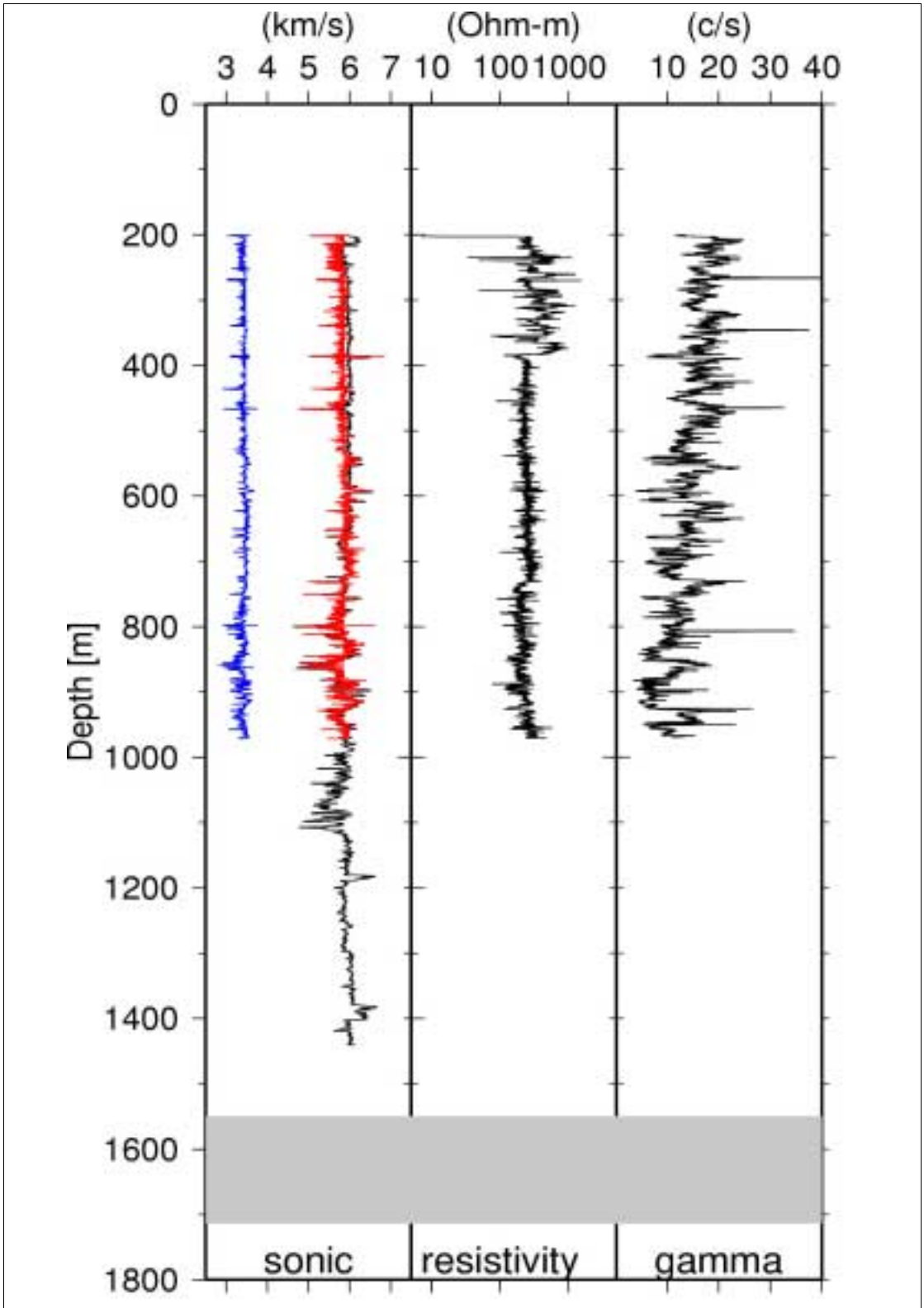

Figure 4−1*. Panel 1: Vp (red) and Vs (blue) velocities calculated from the full−waveform sonic, previously acquired SKB Vp log shifted by −0.4 km/s (black). Panel 2 resistivity log. Panel 3: Natural gamma log. All logs have been filtered with an 11 point running median filter. Sample interval is about 0.1 m.*

5. VSP objectives

5.1. General objectives

The main objectives of VSP are to:

- Locate both sub−horizontal and inclined reflectors in the boreholes
- Detect and locate sub−horizontal reflectors below the bottom of the boreholes
- Detect and locate inclined reflectors not intersecting the boreholes
- Identify in the above categories reflectors possibly not observed on the surface seismic
- Allow better depth conversion of surface seismic data

5.2. Laxemar 2000 experiment

Main goals for the present experiment were to:

1. Image reflectors that are interpreted to intersect the borehole on the surface seismic data and determine the location in the borehole where they intersect and the source of the reflectivity
2. Image reflectors which are not observed on the surface seismic
3. Study the reflectivity of interpreted fracture zones from wireline logs and core data
4. Study the signal penetration depth of the dynamite sources used in the surface seismic acquisition. The dimensions and charge sizes used in the VSP were those that are considered the optimum for surface seismic profiling
5. Compare the signal penetration depth of dynamite with the mechanical SIST source
6. Determine the average velocity as a function of depth for improved depth conversion of the surface seismic data

6. VSP acquisition

6.1. General

VSP data were acquired with the above objectives (chapter 5) in mind in October 2000 over a 9−day period. Detailed information on the source coordinates can be found in Appendix A−2. Table 6−1 provides a summary of the various source points with a brief description of the objective of the source points. Shot point 1 was located near the wellhead of KLX02 whereas the others were offset from about 125 m to about 450 m (Figure 6−1).

Table 6−1. Summary of source points used in the VSP.

Source number	*Shot Point (SP)*	*Source type*	*Recording depths (m)*	*Objective*
1	1	15 grams bedrock	200−1355	Record near zero−offset data for velocity determination, signal penetration studies and imaging of reflectors near the borehole.
2	1	SIST 1000 bedrock	200−1355	Record near zero−offset data for velocity determination and signal penetration studies. Compare mechanical source with dynamite.
3	1	SIST 50 bedrock	200−275, 320−515, 560−595, 680−715, 840−875	Test SIST 50 source and its penetration depth.
4	2	75 grams sediment	200−235, 320−355, 440−475, 560−595, 680−715, 800−835, 920−955, 1040−1075, 1160−1195, 1280−1315	Test the signal penetration for dynamite fired in sediments and compare with bedrock shots.
5	2	SIST 1000 sediment	200−235, 320−355, 440−475, 560−595, 680−715, 800−835, 920−955, 1040−1075, 1160−1195, 1280−1315	Test the signal penetration for the SIST 500 on sediments and compare with other sources
6−9	4−7	SIST 1000 bedrock	200−1355	Provide images of reflectors away from the borehole and possible correlation with surface seismic
10	1	SIST 50 bedrock (acquired in casing)	37.5−195 (2.5 m spacing)	Provide images of the A reflector on the surface seismic which is believed to represent a highly conductive fracture zone.

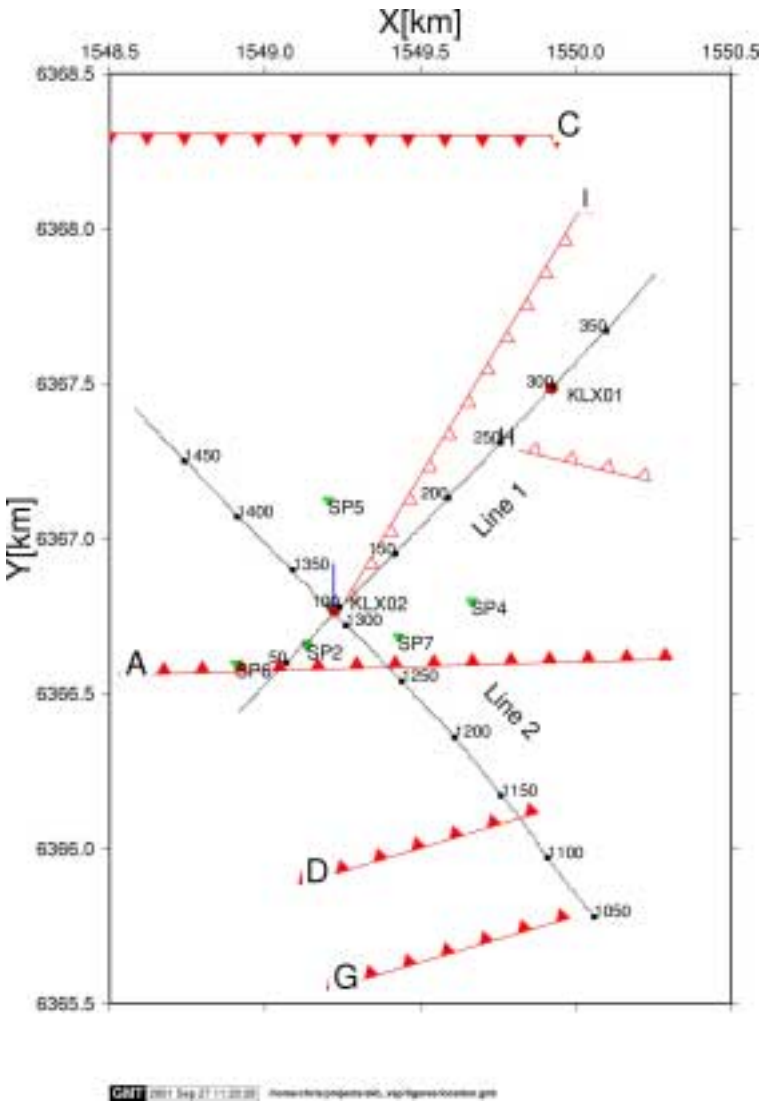

Figure 6−1*. Location of VSP source points relative to the surface seismic reflection profiles. Filled red triangles mark where reflectors observed on the surface seismic intersect the surface, open triangles indicate other possible reflectors. A detailed location map is shown in Figure 6−2.*

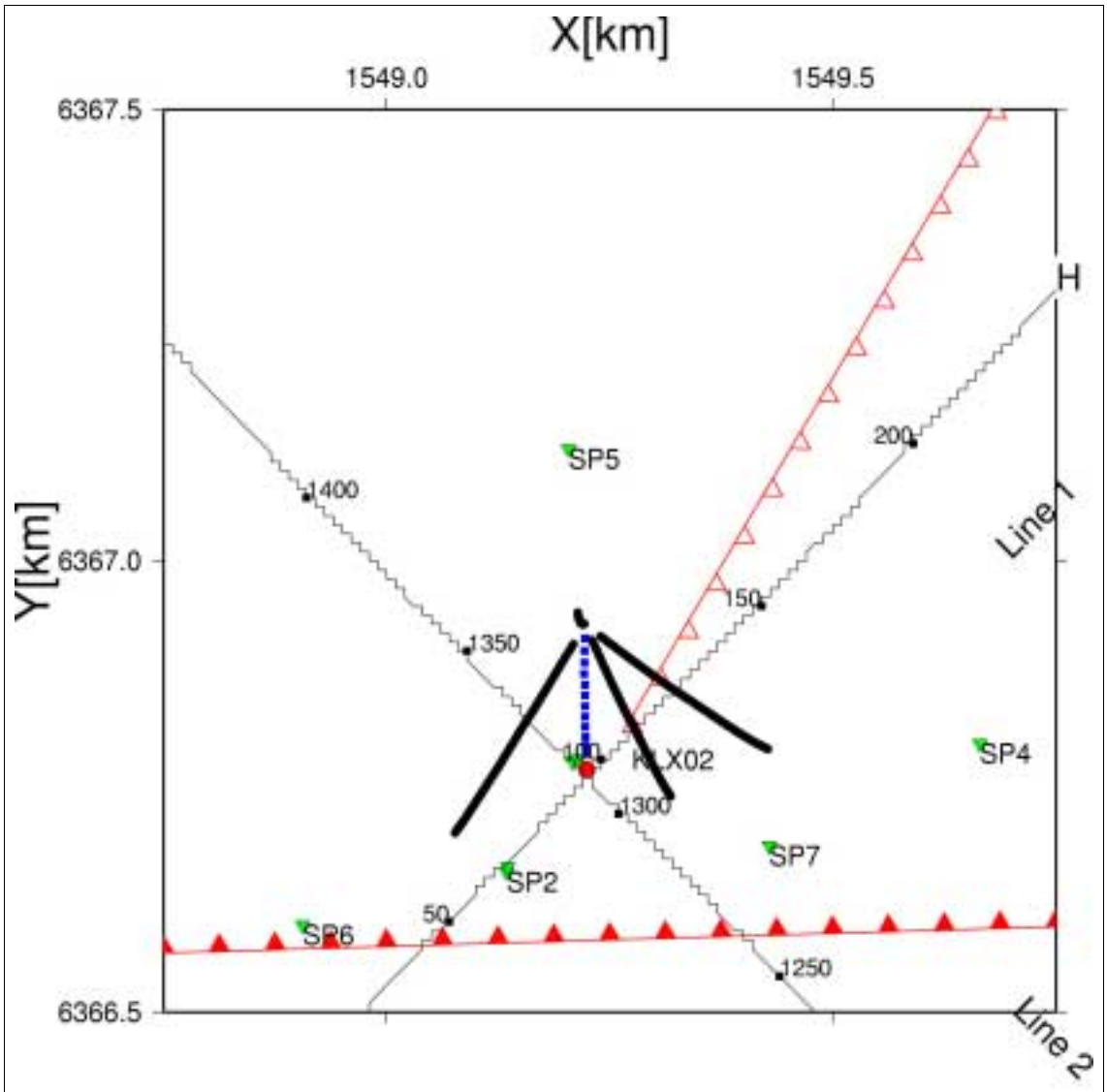

Figure 6−2*. Detailed location map of the source points (inverted green triangles), seismic lines and interpreted reflectors. SP 1 is located close to the KLX02 borehole (red dot). The blue squares show the location of the borehole every 100 m along the VSP survey. The black heavy lines show reflection points for a horizontal reflector at 1400 m depth for SPs 4−7.*

6.2. Procedure

The mobilization started 15.10.2000 from Helsinki to Laxemar. The sonic logging was performed 17.10−19.10 and VSP 20.10−28.10 2000. The demobilization ended 30.10. 2000.

Seismic signals were produced by a VIBRO−SIST (Park et al., 1996) mechanical source (Figure 6−3 and Figure 6−4) and by detonating explosive charges (15 g or 75 g) in shallow shot holes. Two mechanical SIST (Swept impact seismic source) sources were used for the test, a hand−held one (SIST50) and a tractor mounted one (SIST1000).

The mechanical SIST1000 source was a tractor−mounted hydraulic rock−breaker, provided with a computer controlled flow regulator. The tractor with the hydraulic arm and rock−breaking head was rented locally (by SKB). The test was performed with a breaking head model Tamrock Rammer S 27/C, delivering 600−1000 J/impact at 500−1000 impacts/minute. The operating pressure was 80−130 bar. The computer−

controlled flow regulator, command equipment and software were built by Vibrometric specifically for this project. A smaller hand−held electric SIST50 source, delivering only 40−50 J/impact, was also tested.

The pilot signal was transmitted from the source to the recording station by pre−installed cables. The mechanical source is surface coupled. Therefore, outcrops with minimal fracturing and good seismic contact to deeper rock was selected as source stations.

After the functional tests were performed at shallow depth in the borehole, the 8−module 3−component receiver chain (a total of 24 geophones) was lowered to the first (uppermost) measuring level. Each module was clamped independently at 5 m spacing.

Explosive charges were recorded at every level from the bedrock shot point (SP1), but a new shot hole was used only at every third level. For the loose sediment shot point (SP2), data were only recorded at every third level.

Figure 6−3*. SIST50 (left) and SIST1000 sources.*

For control of and guidance to the fieldwork, the data from all channels recorded was decoded (for the VIBRO−SIST source) and checked visually on the display of the seismograph after each shot. Multiple sweeps (2−4) were recorded with the VIBRO−SIST source, in order to reach a satisfactory signal−to−noise ratio. In addition, the data quality was evaluated on site or at a processing office located close to the site, within two days after the measurements. The data quality of the SIST50 source at SP1 appeared poor in the field below 875 m and it was decided to stop recording with the SIST50 below this depth. After final data stacking it was observed that even below this depth it would have been possible to acquire useful data with the SIST50.

Figure 6−4*. SIST1000 source*

The modules in the receiver array contain down−hole preamplifiers with gain set at 34.2 dB. A linear response is expected in the 60 − 4000 Hz band. The modules are equipped with side−arms for clamping (Figure 6−5) that are activated by DC motors and measure the velocity in three orthogonal directions. The clamping control is independent for each module. The z−component is directed along the hole and the x− and y−components are perpendicular to the z−component and to each other. The distance between levels was 5 m, except for source number 10 (Table 6−1) which was recorded in the casing at 2.5 m intervals.

Figure 6−5*. The R8−XYZ−43G receiver chain.*

7. VSP processing

Prior to wavefield processing of the VSP data it is necessary to preprocess the recorded SIST data in order to transform these to the result that would be obtained from a single impact. These preprocessed data are referred to as "raw" sections, although considerable preprocessing has been applied. The preprocessing methodology is described in Appendix A−3. Vertical component sections with only minor processing of the "raw" are shown in Figure 7−1. The lines marked A, Ba, B, Bb, D, G, and E represent the locations in the KLX02 borehole where these reflectors, as interpreted on the surface seismic, are projected to intersect the borehole (see Figure 6−1for the reflector orientation on the surface seismic).

The "raw"data shown in Figure 7−1 were processed both by Vibrometric Oy and Uppsala University. These "raw" data are the basis for the analysis and interpretations presented in this report.

7.1. Uppsala processing

The data were processed in Uppsala with standard methods using the seismic processing package ProMAX (Table 7−1). The processing was kept basic so as not to introduce any artificial reflections into the processed sections. After initial processing, the first set of steps (steps 9−14 in Table 7−1) were designed to equalize the frequency content in the data and to compensate for the 20 ms shot delay. The most dominant events at this stage of the processing are the downgoing P− and S−waves from the source (Figure 7−2). In addition to the direct downgoing P− and S−waves, downgoing converted S−waves are also present, the strongest conversion being at about 200 m on SP 1. Some weak upgoing reflections may also be observed in Figure 7−2. In order to better see these reflections, the downgoing P− and S− (both direct and converted) waves were removed by velocity filtering (Figure 7−3 to Figure 7−6) After removing the downgoing P−waves it becomes clearer where downgoing S−waves are generated along the borehole and where reflected waves intersect the borehole (Figure 7−3 and Figure 7−4). After removal of downgoing S−waves (Figure 7−5 and Figure 7−6), it is primarily reflected waves that are left in the sections, aside from tube waves and processing artifacts. However, as discussed earlier, it is not obvious if the reflected waves are direct P−wave reflections or converted PS−wave reflections. This point will be further illustrated later in section 8.4.

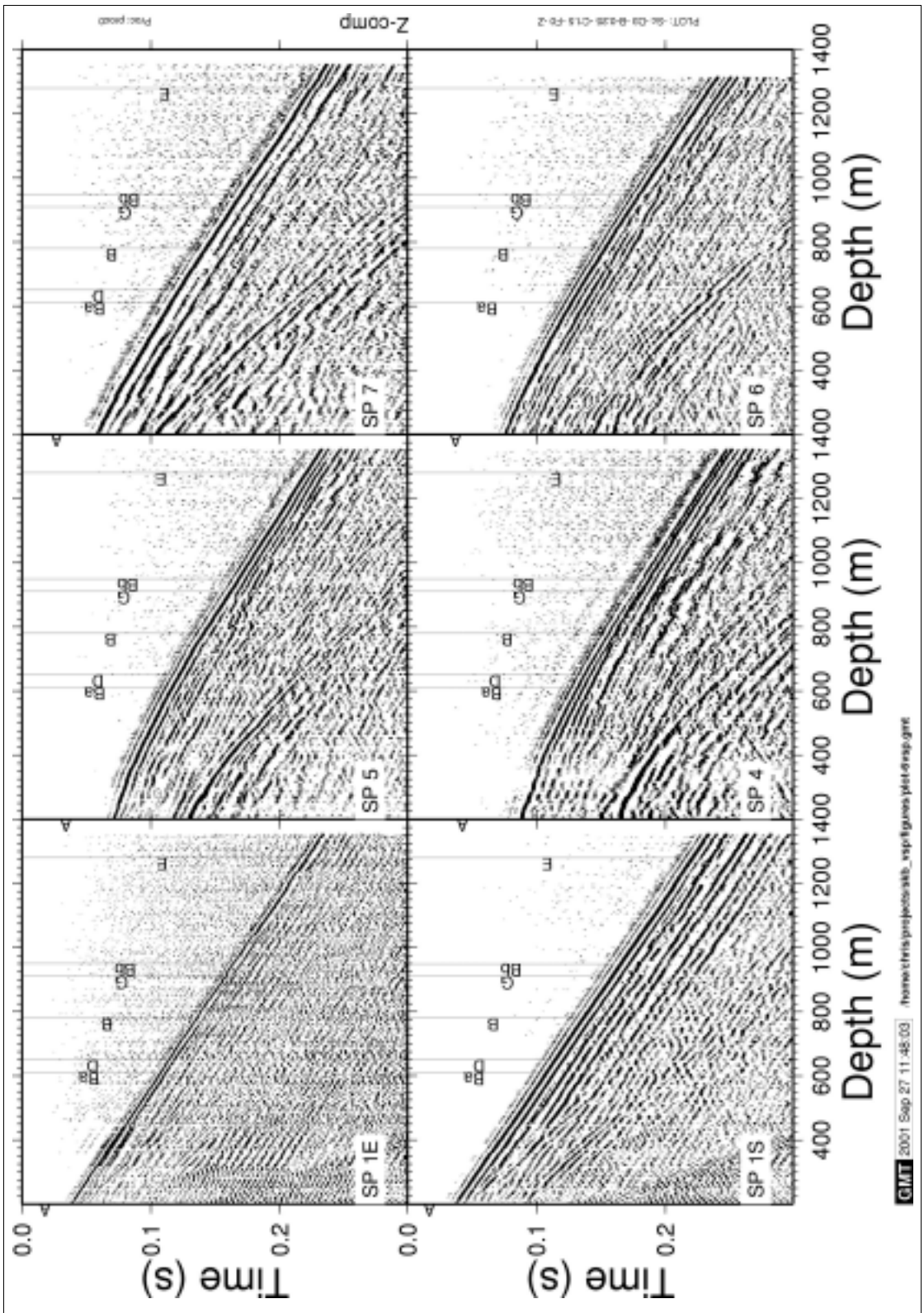

Figure 7−1*. VSP data processed to step 9 in Table 7−1.*

Table 7−1. Processing steps used by Uppsala.

Step	***Process***
1	Read SEG2 data
2	Resample to 0.5 ms
3	Apply shot delay static shifts
4	Rotate horizontal components to radial and transverse orientation to source
5	Scale by $t^{1.0}$
6	Bandpass filter 40−60−300−450 Hz
7	Trace equalization: 0:20−220/ 1800:320−520/ (distance:window)
8	Kill poor traces
9	In−fill killed traces
10	Spectral whitening: 60−80−240−300 Hz
11	Bandpass filter: 60−90−270−400 Hz
12	FX−Decon: 1−300 Hz, size 20/11 (traces/samples)
13	Mute data prior to first arrivals
14	Trace equalization: 0:20−220/ 1800:320−520/ (distance:window)
15	Remove downgoing P−waves: 15/1/6000 (traces/samples/velocity)
16	Bandpass filter: 40−60−300−450 Hz
17	Mute data prior to first arrivals
18	Trace equalization: 0:20−220/ 1800:320−520/ (distance:window)
19	Remove downgoing S−waves: 9/3/3460 (traces/samples/velocity)
20	Bandpass filter: 40−60−300−450 Hz
21	Mute data prior to first arrivals
22	Trace equalization: 0:20−220/ 1800:320−520/ (distance:window)

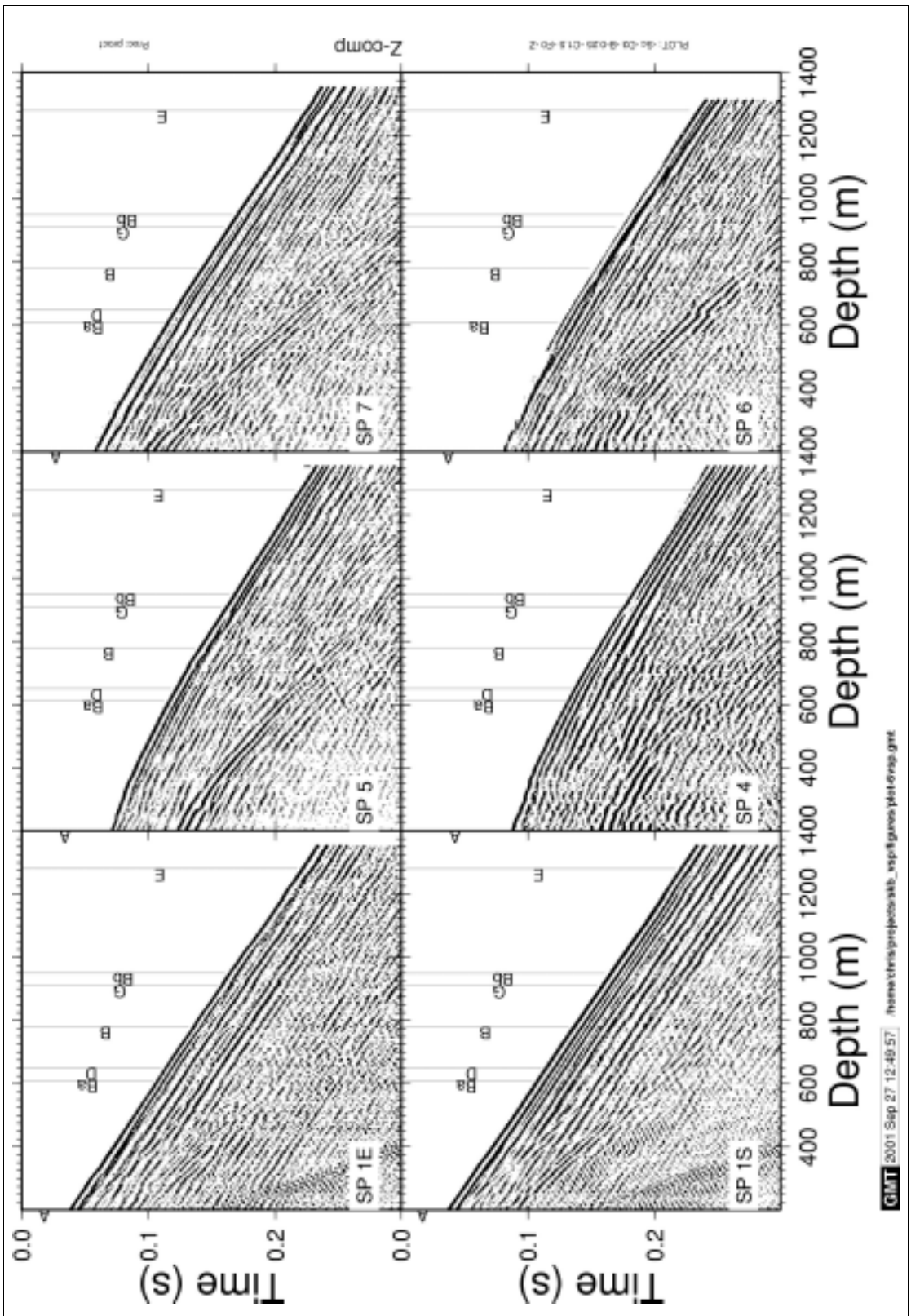

Figure 7−2*. Vertical component VSP data processed to step 14 in Table 7−1.*

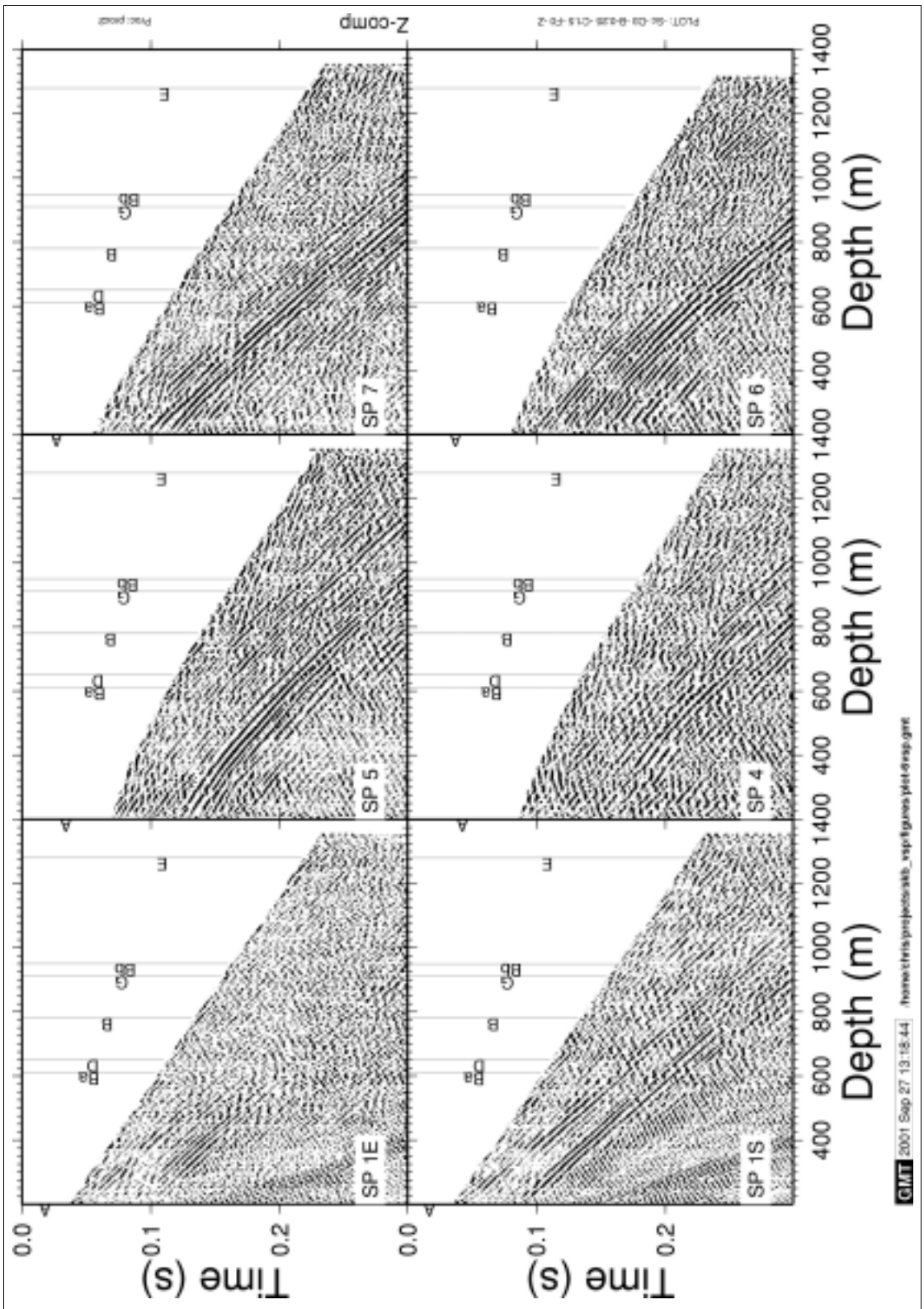

Figure 7−3*. Vertical component VSP data processed to step 18 in Table 7−1.*

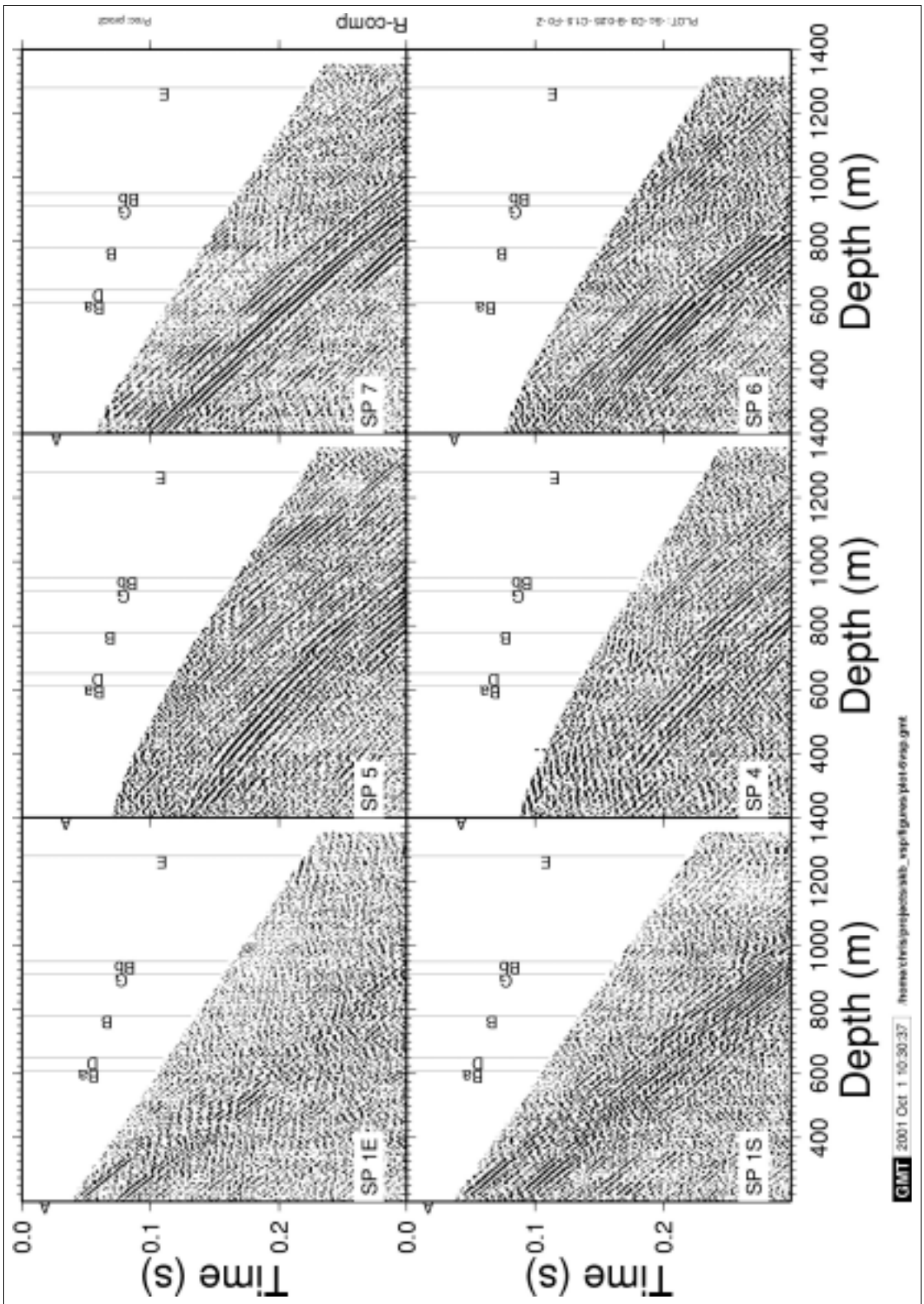

Figure 7−4*. Radial component VSP data processed to step 18 in Table 7−1.*

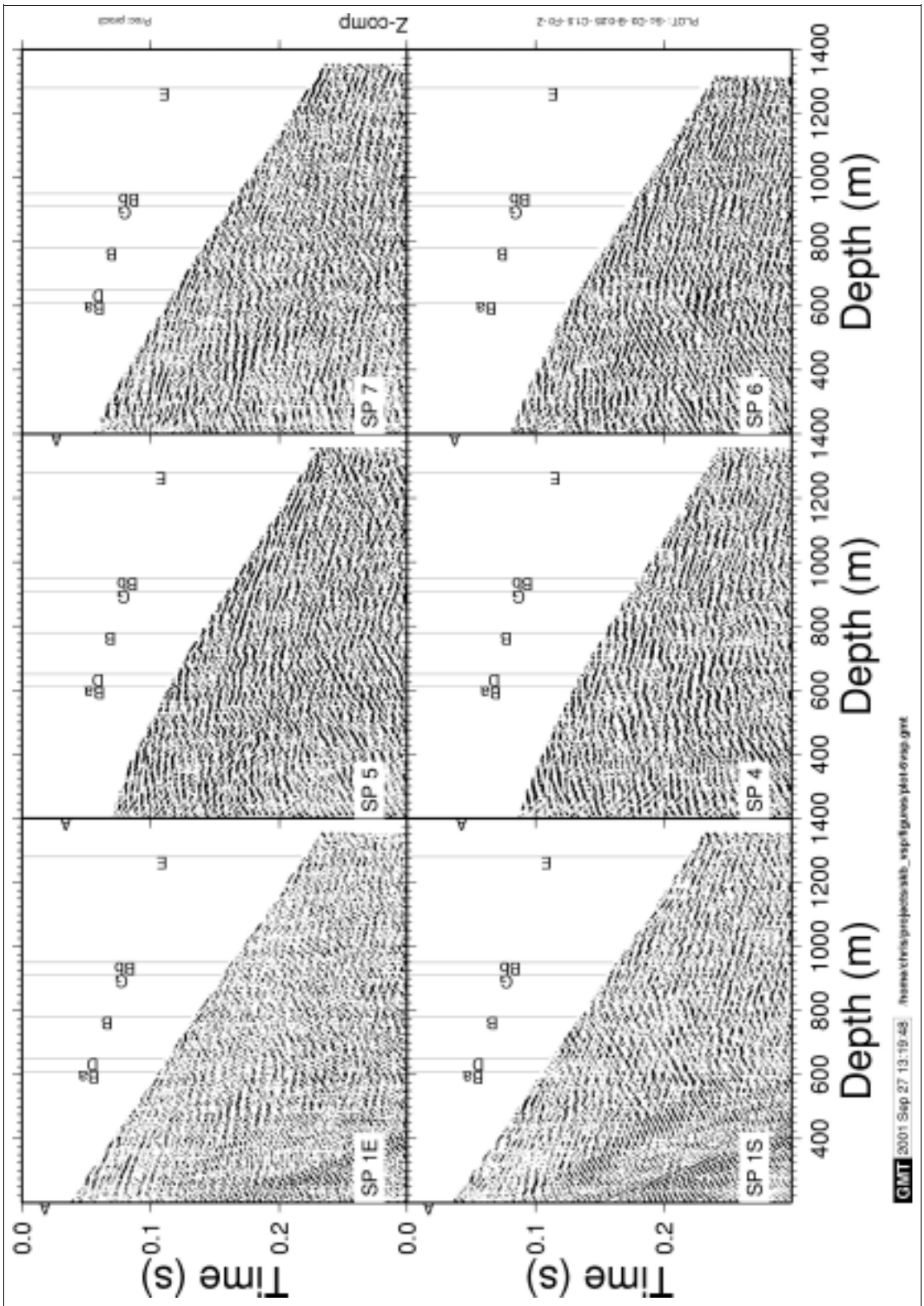

Figure 7−5*. Vertical component VSP data processed to step 22 in Table 7−1.*

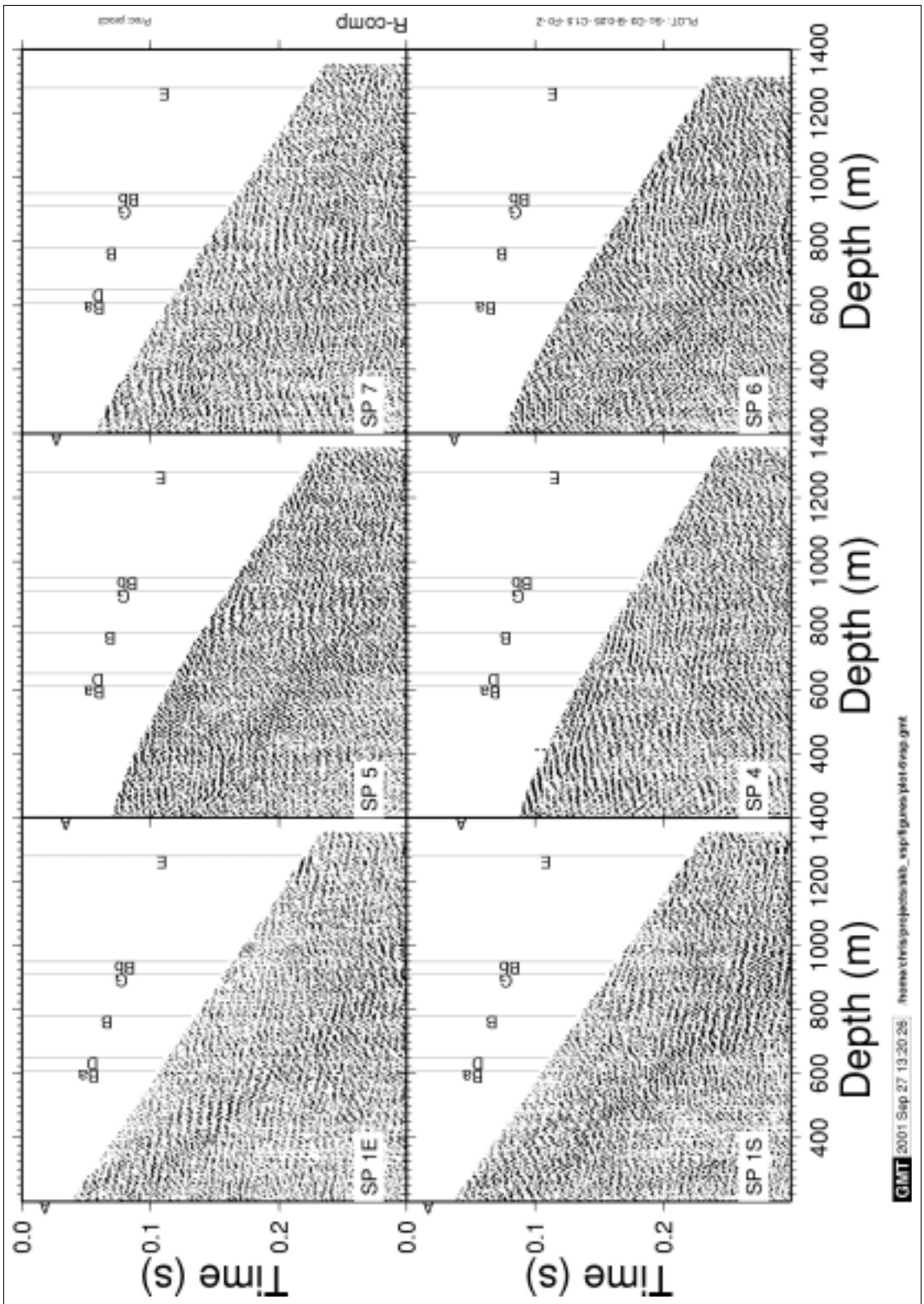

Figure 7−6*. Radial component VSP data processed to step 22 in Table 7−1.*

7.2. Vibrometric processing

Lithological contacts, faults, fracture zones and dissolution features may all reflect seismic waves. Reflections from faults and fracture zones are usually weak and extensive processing is needed to obtain information on the position of the reflectors from the seismic profiles.

The first step of the processing is to improve the signal−to−noise ratio, so that the later events, e.g. reflections, become visible. For this, criteria for discriminating between signal and noise have to be determined. As the reflection coefficients are expected to be weak, the reflectors cannot be identified by amplitude contrast alone. Phase consistency is a much more sensitive indicator, but must be used with caution. There is always a degree of coincidental coherency in the data, which may create artifacts, in the absence of true events. If the data quality is poor this can result in over processed images.

The purpose of the preliminary processing is to remove disturbances and adjust the signal levels in such a way that the amplitudes of different traces and different parts of the same trace are comparable.

The initial processing steps applied by Vibrometric Oy differed slightly from those of Uppsala in the choice of velocity filters, frequency filters, etc. The pre−processing sequence used to enhance the signal−to−noise ratio was:

- Data correlation,
- Data stacking,
- Picking of the first arrival times,
    - Velocity determinations: − The seismic P−wave velocities at the survey area were determined from the travel times of the first arrivals (the average velocity is 5850 m/s),
    - Determination of the orientation of the horizontal X and Y components. Rotation of the horizontal components to Radial and Transversal components,
- Band pass filtering between 40 Hz and 300 Hz,
- Removal of direct P− waves using median filtering,
- Removal of down−going S−waves using median filtering,
- Removal of tube waves using median filtering,
- Amplitude compensation using AGC. Amplitude compensation (AGC) is performed to cancel the effects of geometrical spreading and attenuation.

Due to the free rotation of the down−hole probe while changing the depth, the horizontal components (X and Y) show poor coherence in both amplitude and phase. Therefore, the horizontal components were rotated for each level so that, after rotation, one horizontal component points to the source and will be called the radial component (R). The other component becomes transversal (T). The R, T and Z components are perpendicular to each other and the Z−component is directed along the borehole.

The reflections from faults and fracture zones usually display relatively weak seismic characters and extensive processing is needed to obtain information on the position of the reflectors from the seismic profiles.

The first stage of the processing sequence focuses on eliminating such wavefields as the direct P, direct S, tube−waves and ground−roll, so that the weaker later events, e.g.

reflections, become visible. In this stage, the direct wavefields and other coherent disturbances are removed by slant median filtering and the signal levels are adjusted in such a way that the amplitudes of different traces and different parts of the same trace become comparable.

The second stage of the processing sequence consists of:

- Picking of the first arrival times and velocity analysis;
- Rotation of the horizontal components to radial and transverse, where "radial" stands for the direction perpendicular to the hole and pointing towards the source and "transverse" for the direction perpendicular to the radial and to the hole;
- Image Space (IP) processing− to enhance the reflected wave fields and separate reflection events originating at interfaces with different orientations (a description of Image Space technique is given in Cosma and Heikkinen, 1996).

Figure 7−7 shows the final image processed sections which are the basis for picking reflected waves and orienting the reflectors in 3D.

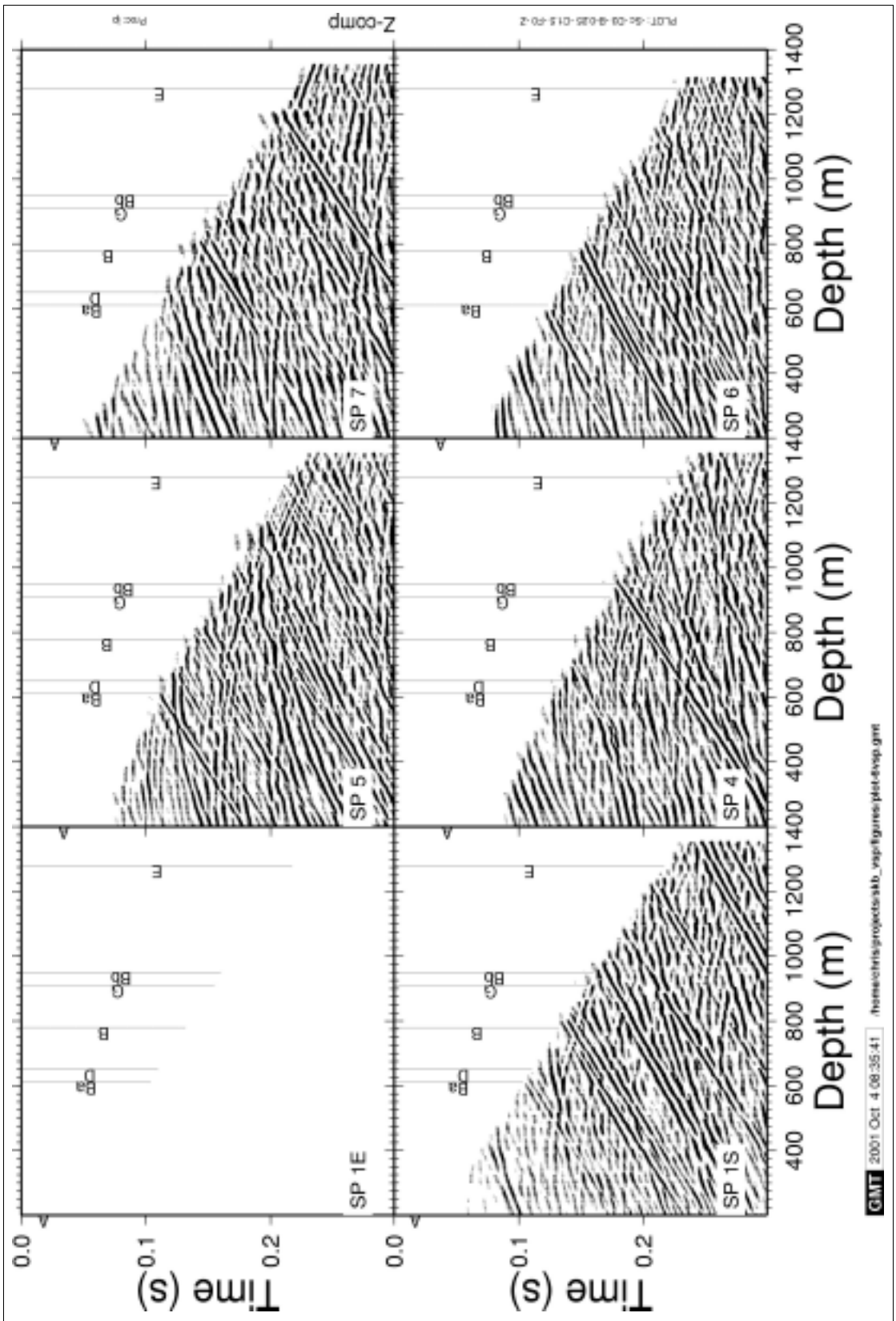

Figure 7−7. *Image point processed sections which form the basis for the Vibrometirc Oy reflection picks and interpretation. The explosive data from SP1 was not processed.*

8. VSP results

8.1. Velocity functions

Knowing the average velocity as a function of depth in an area is important for estimating the dip and depth to a reflector from surface seismic data. Table 8−1 illustrates this point showing that the estimated depth may vary from less than 700 m to more than 800 m using reasonable velocities and apparent dip. For reflectors that dip more steeply the estimated depths to a reflector will vary even more. By measuring the time for the direct P−wave to travel from the source point to the receiver point and knowing the distance an average velocity for the rock can be calculated (Figure 8−1). The average velocity estimated from all source points starts at about 5.6 km/s at 200 m, increasing to about 5.8 km/s at 800 m and remaining at this level to about 1100 m, and then increasing again to about 5.9 km/s at the bottom of the survey. It is this velocity function that should be used to estimate dips and depths to reflectors.

Average velocities may be biased to low values if a low velocity layer is present in the the near surface. In order to avoid this bias, interval velocities may be calculated based on various methods. Two methods have been applied here. The first one is based on first arrival times where interval velocities are calculated by dividing the time difference in the first arrivals from two depths by the difference in distance traveled. The second method is based on aligning the first arrivals at varying trial velocities over the fixed 8−module 3−component array used in the acquisition. The distance between the receivers is known accurately over these 35 m sections and a good estimate of the apparent velocity over the array may be obtained. When the direct P−wave is propagating parallel to the borehole, as for SP 1, this apparent velocity will be close to the interval velocity.

Table 8−1. Estimated dips and depth to a reflector for varying average velocity and given two way time (T) and apparent dip (DT/DX).

V(km/s)	*T(ms)*	*DT/DX(ms/km)*	*Dip*	*Z(m)*
5.7	200	200	34.8	694
6	200	200	36.9	750
6.3	200	200	39.1	811

When comparing the VSP interval velocities, as well as the full waveform sonic logging velocities acquired in October 2000, with the previously acquired SKB sonic log it is clear that there is a problem with the SKB sonic log (Figure 8−1). The average sonic velocities are much higher, by about 0.4 km/s, than the VSP velocities. The same is true for the full−waveform sonic acquired in this study compared with the previous sonic log acquired by SKB (Figure 4−1), with the SKB sonic log being about 0.4 km/s higher. The reason for this is unclear, but needs to be investigated. Any depth conversion of the surface seismic using the SKB sonic log would result in large errors. Note, that the locations of low velocity zones in the SKB sonic and the full−waveform sonic appear to correlate well (Figure 4−1) indicating that the SKB sonic log can be used for determining where fracture zones are located.

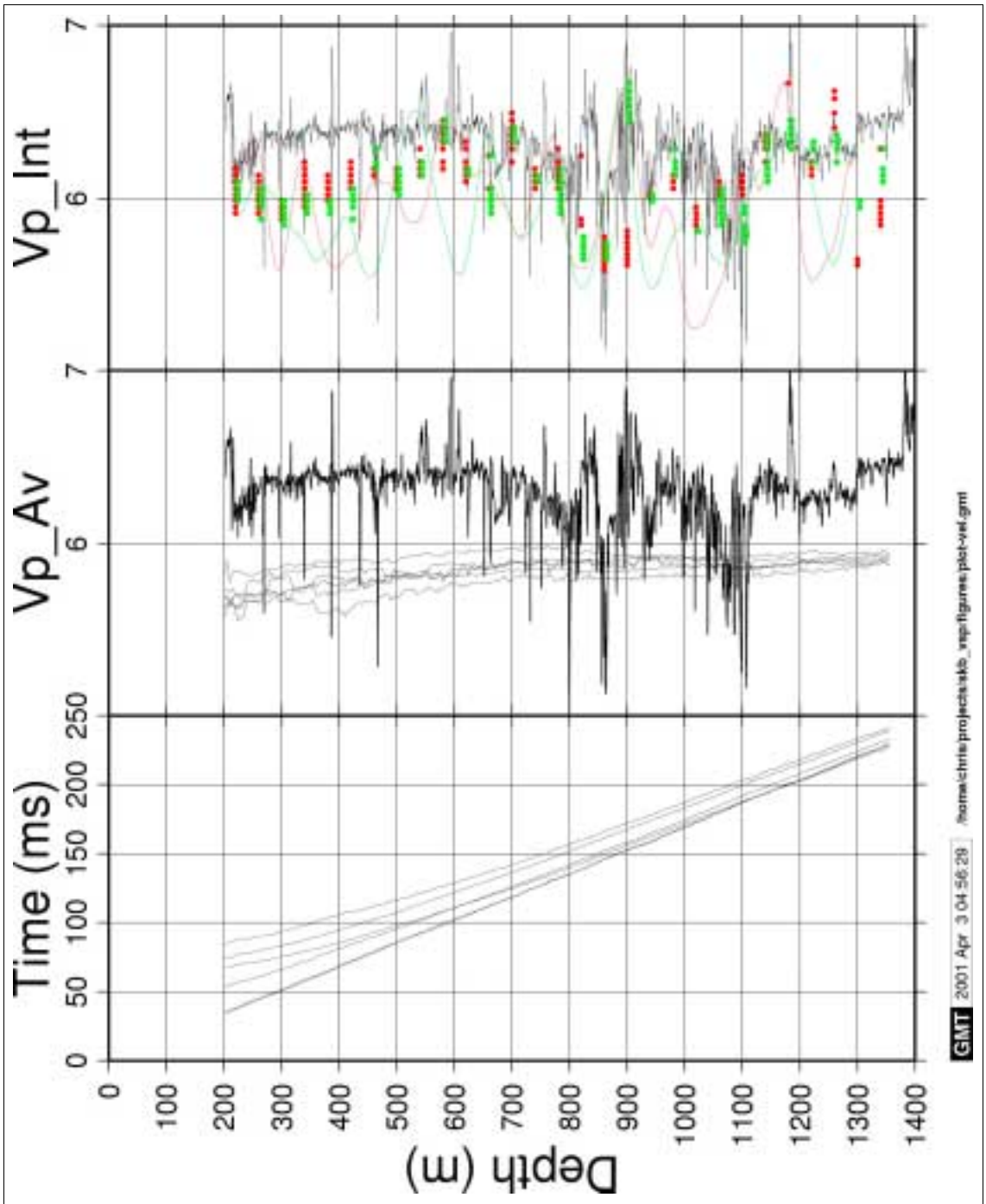

Figure 8−1*. First break travel times and velocity functions. Green implies the data are from VSP source SP1 and red implies the data are from VSP source SP2. Interval velocities have been calculated over 50 m depth intervals (lines) and over the 35 m fixed arrays (dots) for SP1 and SP 2.*

8.2. Signal penetration

Maximum amplitudes were picked in a 15 ms window after the first break in order to study the signal penetration of the various sources (Figure 8−2). Higher amplitudes are generally recorded from the SIST1000 bedrock source compared to the dynamite bedrock source. Note that there is more variability in the recorded amplitudes from the dynamite source. This is most likely due to variations in source coupling and near

surface conditions, in spite of all shot holes being located on the same outcrop. The variability of the recorded amplitude from the 75 gram sediment dynamite source is even more. Sometimes these shots have the highest amplitudes at a given level and sometimes they are the lowest. The SIST1000 sediment source shows much less variability in recorded amplitudes.

At a mean impact rate of 10/s and a mean energy/impact of 400 J, the energy produced by the SIST1000 in 1 second, i.e. the mean power, is 4 kJ/s. The fraction that is radiated elastically depends upon, among other factors, the ground quality in the immediate vicinity of the impact point. We can estimate the elastic energy generated to be from 0.25 to 0.5 of the total energy. Therefore, the net output is 1 to 2 kJ/s for the SIST1000 source used in this study. Similar reasoning gives a net output of 0.1 to 0.2 kJ/s for the SIST50 source (energy/impact is 48 J). Dynamite delivers approximately 4 kJ/gram, as total heat output. The fraction of the energy radiated elastically is from 0.1 to 0.2, which gives a net output of 0.4 to 0.8 kJ/gram. Based on these values the total amount of radiated elastic energy may be estimated from the various sources (Table 8−2).

Table 8−2. Comparative estimates of source energy.

	SIST1000 30s sweep		***SIST50 30s sweep***		***Dynamite 15g***		***Dynamite 75g***	
Gross Energy Output (kJ)	120		12		60		300	
Estimate	Low	High	Low	High	Low	High	Low	High
Elastic/Total Energy Ratio	0.25	0.5	0.25	0.5	0.1	0.2	0.1	0.2
Net Elastic Energy Output (kJ)	30	60	3	6	6	12	30	60

Based on Table 8−2, expected measured amplitudes for the bedrock dynamite source should be about 2 times less than for the SIST1000 source (amplitude should be proportional to the square root of the net energy). This is in agreement with observed amplitudes from the dynamite source which are, on average, about half of those observed from the SIST1000 bedrock source (Figure 8−2).

The SIST1000 sediment source does not show the same amplitude decay as the SIST1000 bedrock source. At shallower levels, considerably lower amplitudes are recorded, while at deeper levels the amplitudes are comparable. This may be explained by the difference in ray paths near the surface. At shallower levels, the offset sediment source rays must travel through more attenuating near−surface bedrock, while at the deeper levels the ray paths pass through nearly the same rock section as those from the bedrock source location.

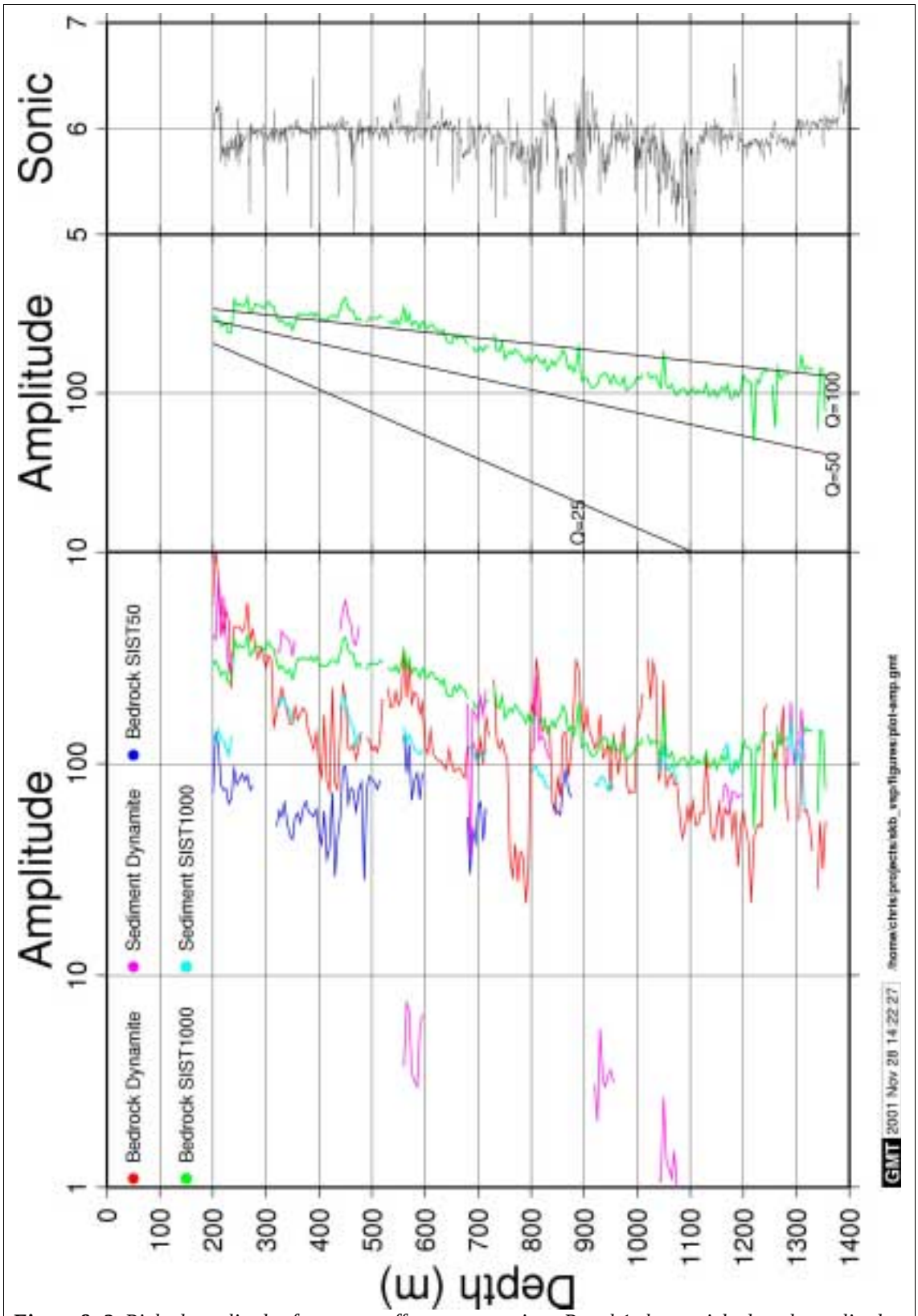

Figure 8−2*. Picked amplitudes from near offset source points. Panel 1 shows picked peak amplitude of the first arrival for all near offset source points, panel 2 shows the picked amplitude for the SIST1000 source on bedrock and theoretical amplitude decay curves for various values of Q (seismic attenuation), panel 3 shows the sonic velocity.*

The recording with the SIST50 was stopped at a depth of 875 m. However, elaborate signal enhancement procedures applied during processing revealed that the data quality at that depth was relatively good. By extrapolation and comparison with the SIST1000 data it could be determined that the SIST50 could have produced usable VSP records to a depth in excess of 1000 m. The ratio of the amplitudes of the two sources at the same source and receiver locations was approximately 3, which roughly corresponds to the square root of the energy ratio, as shown in Figure 8−3. Likewise, comparable amplitudes were obtained for source−receiver distances 3−fold larger for the SIST1000 than for the SIST50.

It can be concluded that the investigation depth of the SIST1000 is at least 3−fold the one of the SIST50, i.e. 3000 m. A larger depth range could be achieved, if desired, by increasing the power of the breaker and/or the number of sweeps added to the same record.

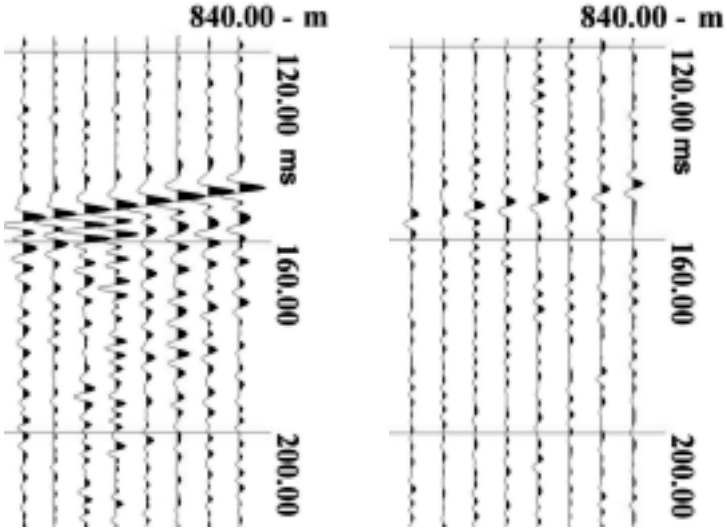

Figure 8−3*. SIST1000 vs. SIST50.*

The SIST1000 bedrock source has a consistent amplitude decay curve with depth allowing Q (seismic attenuation) to be estimated (Figure 8−2). Comparison of constant Q amplitude decay curves (for an average frequency of 160 Hz and velocity of 6000 m/s) in panel 2 in Figure 8−2 shows that Q lies somewhere between 50 and 100, probably closer to 100. A value of 100 implies that the amplitude of a seismic wave will be reduced by a factor 2.718 after propagating a distance of 100 wavelengths. At a frequency of 200 Hz and a velocity of 6000 m/s, 100 wavelengths corresponds 3000 m.

8.3. Reflector imaging

One of the most important aspects of VSP is the identification of reflectors and determining their orientation and where they intersect the borehole. The processed VSP sections from KLX02 show numerous reflections and it is somewhat difficult to identify which ones are important. If reflections can be correlated from at least three shot points then it is possible to determine their orientation. A visual inspection of the sections shows that reflections originate from 3 groups:

Group 1: Sub−horizontal to gently dipping reflectors with varying dip

Group 2: Moderately dipping reflectors with two sub−groups, one with NNW dips and the other with SSE dips

Group 3: Steeply SE dipping reflectors with strikes of 50−70°

The main reflections from these groups are listed in Table 8−3. Note that these reflections were picked by Vibrometric Oy independently of the surface seismic data based on the sections shown in Figure 7−7. Depending on the direction of incidence of the incoming wave and the reflecting boundary, PP and/or PS reflections can be generated. Processing/interpretation ambiguities may appear e.g. due to the interpretation of PS reflected conversions as PP reflections. The result is that the corresponding reflector may be interpreted as having a different dip than its real one. The strategy applied for avoiding such errors has been based on trial fits for each identified event with both PP and PS time functions. For the picked events, only PP reflections have been identified. Examples of the picked events from SP1 are show in Figure 8−4. An example of how reflector 2 correlates from shot point to shot point is shown in Figure 8−5. A perspective view of the reflectors is shown in Figure 8−6 where the size of the reflector corresponds to the area over which reflections are observed from it.

Table 8−3. Main reflectors on VSP as picked by Vibrometric Oy. Origin B, E , D and G events can be correlated to the surface seismic data while origin K and L events are not observed on the surface seismic data.

Reflector	*Strike*	*Dip*	*Depth (m)*	*Group*	*Origin*
16	195	15	620	1	B
8	261	11.5	760	1	B
2	52	19	800	1	B
3	15	17	939	1	B
1	300	10.5	940	1	B
15	195	15	1100	1	B
6	97	16	1200	1	E
12	98	23	1400	1	E
4	253	42	620	2a	D
9	258	40	840	2a	G
14	55	38	450	2b	K
11	73	40	1165	2b	K
5	54	76	1390	3	L
10	68	75	1475	3	L
13	52	79.5	2200	3	L
7	58	83	3600	3	L

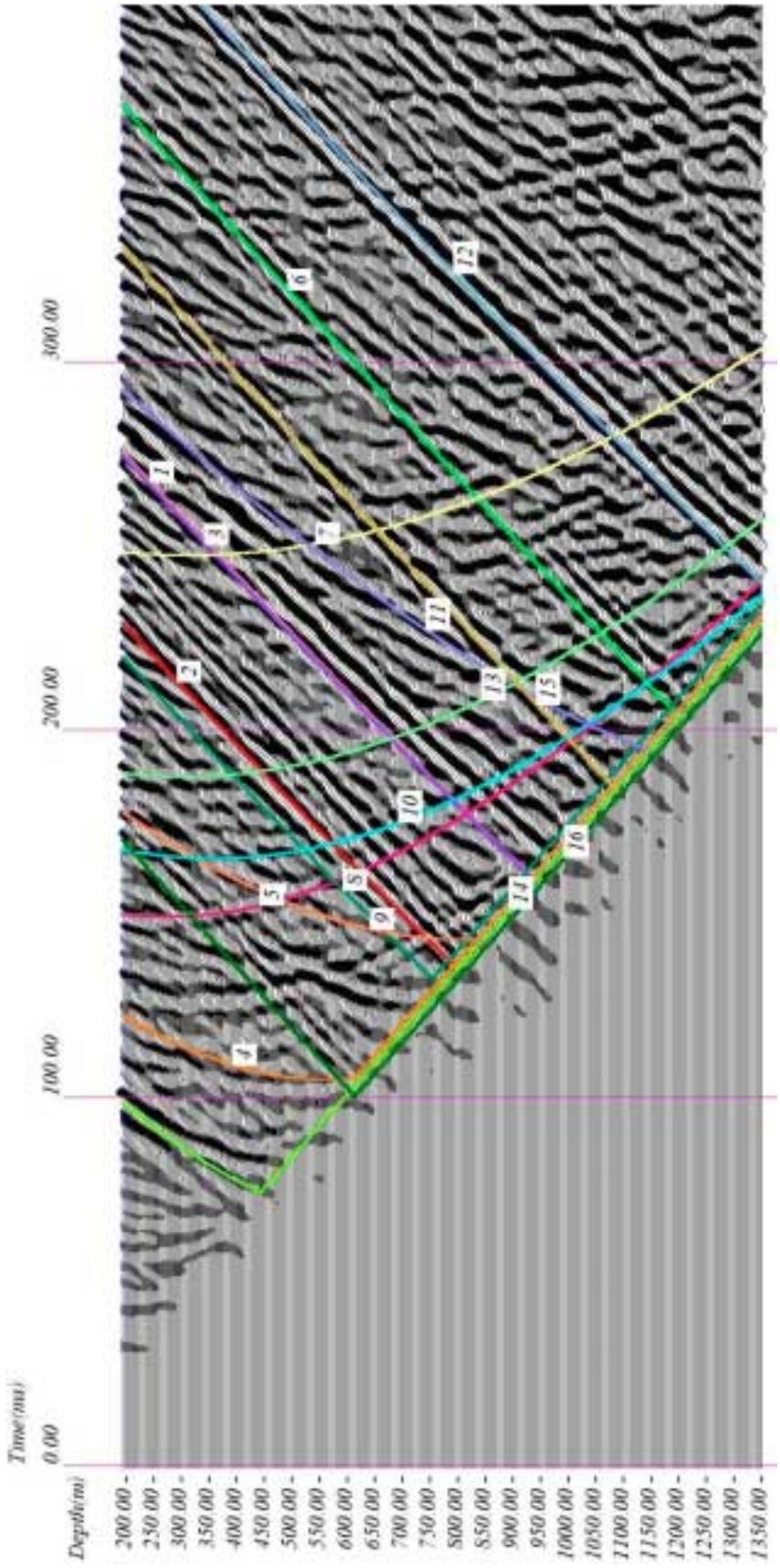

Figure 8−4*. Vibrometric processed mechanical source vertical component data from SP1. Picked events are from Table 8−3 marked.*

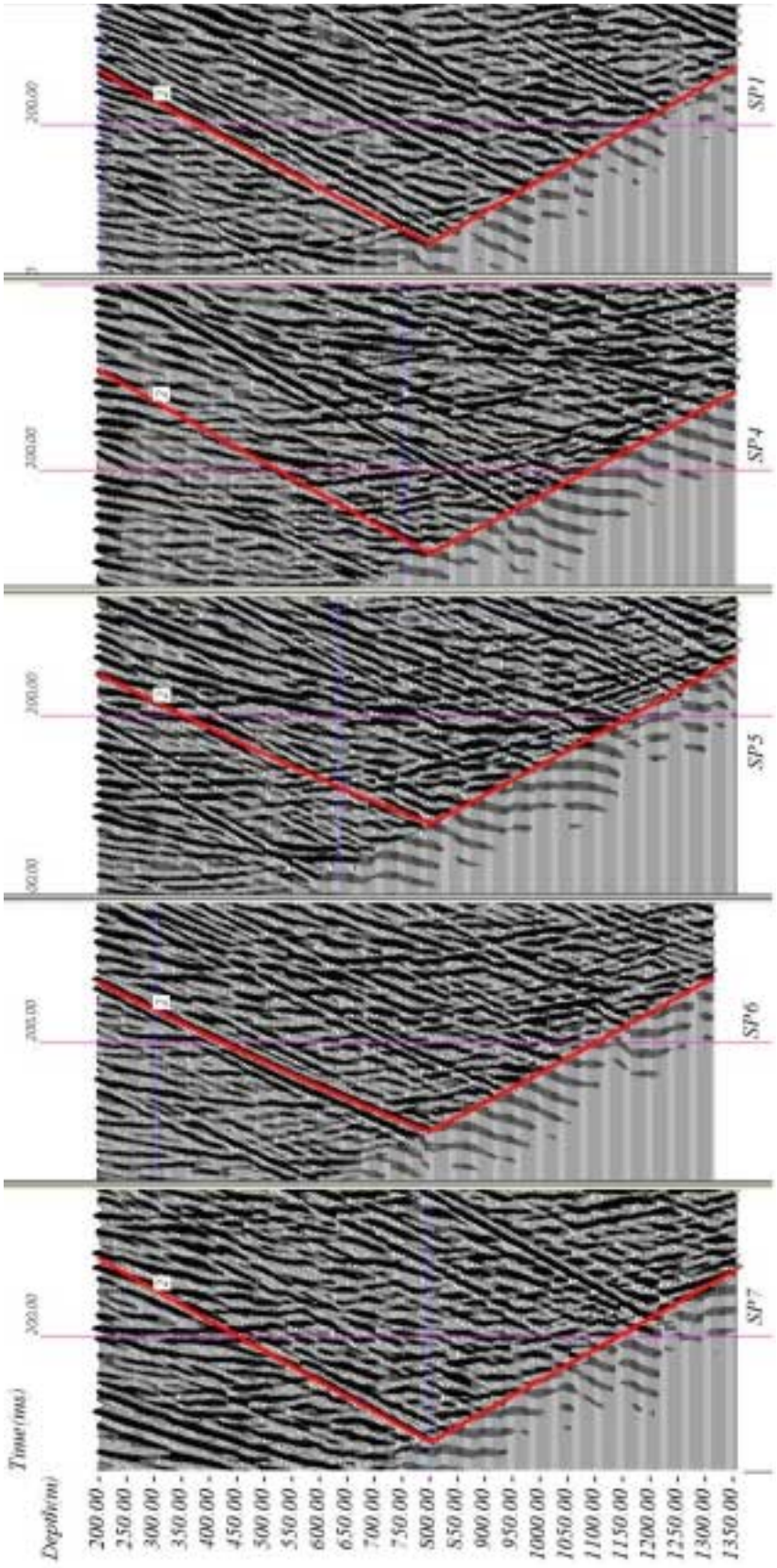

Figure 8−5*. Reflector 2 in Figure 8−4 picks for SP1, SP4, SP5, SP6 and SP7.*

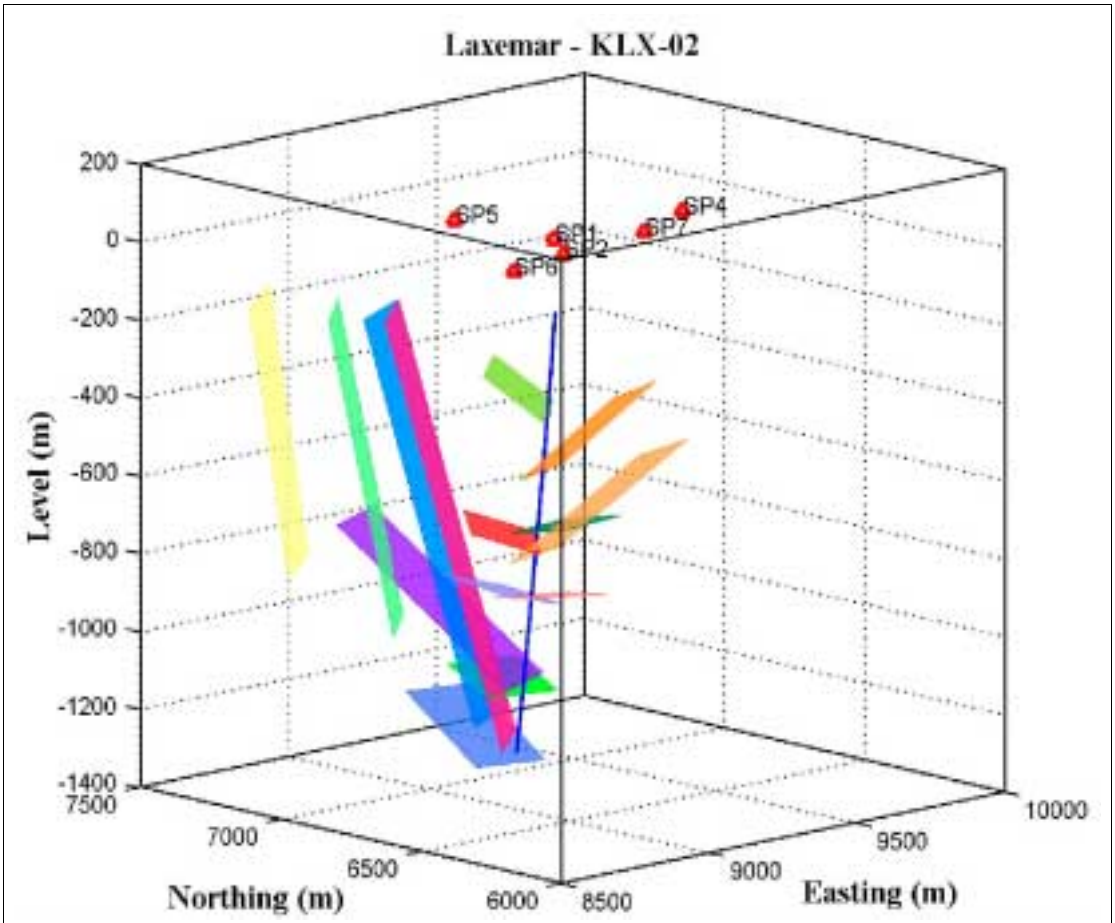

Figure 8−6*. 3D perspective view of picked reflectors by Vibrometric Oy. Colors of reflectors correspond to picks in Figure 8−4. Geometry of reflections are given in Table 8−3 where reflector number is also shown in Figure 8−4.*

A comparison of the reflectors identified on the surface seismic (Table 3−1) to those identified on the VSP (Table 8−3) shows that the group 1 reflections roughly correspond to the sub−horizontal B and E reflections and the group 2a reflections to the moderately dipping D and G reflections (Figure 8−7). The interpreted dips on the VSP data are, however, somewhat greater than on the surface seismic. This may may be due to the reflectors being non−planar resulting in the VSP measuring a local dip and the surface seismic a more regional dip. Neither do these events intersect the borehole exactly where predicted from the surface seismic. This may again be due to the non−planar nature of the reflectors resulting in vertical shifts in the reflectors of tens of meters over distances of 100 m. See section 9.1 for a discussion on the accuracy of locating the reflectors.

Reflections 16, 8, 2, 3 and 1 on the VSP correlate well with the the Ba, B and Bb reflections on the surface seismic and intersect the borehole near greenstones that have significantly higher density than the surrounding rock. This correlation and their sub−horizontal orientation suggest that they originate from the greenstones.

Reflections 6 and 12 on the VSP intersect the borehole close to clear high density

anomalies on the borehole log that correspond to greenstones and are interpreted to originate from these greenstones. They do not correlate well with reflection E on the surface seismic. However, reflection E is not well imaged where the boreholes cross (Figure 3−2) and its projection into the borehole is more uncertain. Therefore, these two events are probably related to reflector E on the surface seismic.

Reflection 15 on the VSP does not correlate with any clear reflection on the surface seismic. However, it does correlate with a low velocity zone at 1100 m that represents the base of the thick fractured interval between 800 m and 1100 m. If this low velocity zone produces reflection 15 then it has a sub−horizontal orientation.

On the VSP, both reflectors 4 (D on the surface seismic) and 9 (G on the surface seismic) intersect the borehole near distinct low velocity zones at 660 m and 840 m, respectively, suggesting that these reflections originate from fracture zones.

Group 2b is not directly observed on the surface seismic (K in Table 8−3). Reflector 11 in this group is almost sub−parallel to reflector C on the surface seismic and may be related to it. However, it does not correlate with any fracture zone on the logs, but rather the high density greenstone at 1180 m. Reflector 14 in this group correlates with a low velocity zone at 460 m, suggesting that it originates from a SE dipping fracture zone. Where these reflections are expected to be observed on the surface seismic is discussed in more detail in section 8.4.

The group 3 steep reflections (L in Table 8−3) are not expected to be observed directly on the surface seismic. However, their southeast dip suggests that their effect on the surface seismic should be most apparent on the NW−SE running surface seismic Line 2. As noted earlier in section 3.2, the reflections are indeed more discontinuous on Line 2 than on the NE−SW running Line 1, suggesting that it is the steep group 3 reflectors which are disrupting the more sub−horizontal reflectors on Line 2. The uppermost of these two reflections intersect the borehole at 1390 m and 1475 m, in an interval with low fracture density and no fracture zones. However, determining the exact point of intersection is difficult for steeply dipping zones and the reflections could intersect deeper in the borehole. If the reflections do intersect the borehole deeper than interpreted, then they may be related to the highly fractured interval between 1550 m and 1700 m. This fracture zone would then dip steeply to the SE.

There are number of steep reflectors intersecting the borehole at shallower levels in addition to the group 3 reflectors picked by Vibrometric Oy. They were not picked by Vibrometric Oy because they are observed on too few traces and not on all shot sections. They are most apparent on the dynamite data from SP1 processed by Uppsala (Figure 7−5), but are also observed on some of the sections from the other shot points. The two most prominent ones intersect the borehole at about 400 m and 600 m. The reflections may be modeled as originating from steeply dipping interfaces with the same orientation as the group 3 reflectors (see section 8.4).

The general strike, dip and location of the group 3 reflections and those intersecting the borehole at shallower depths suggest that these are related to the NE−SW regional fracture zone SFZ04 shown in Figure 3−19 in Ekman (2001).

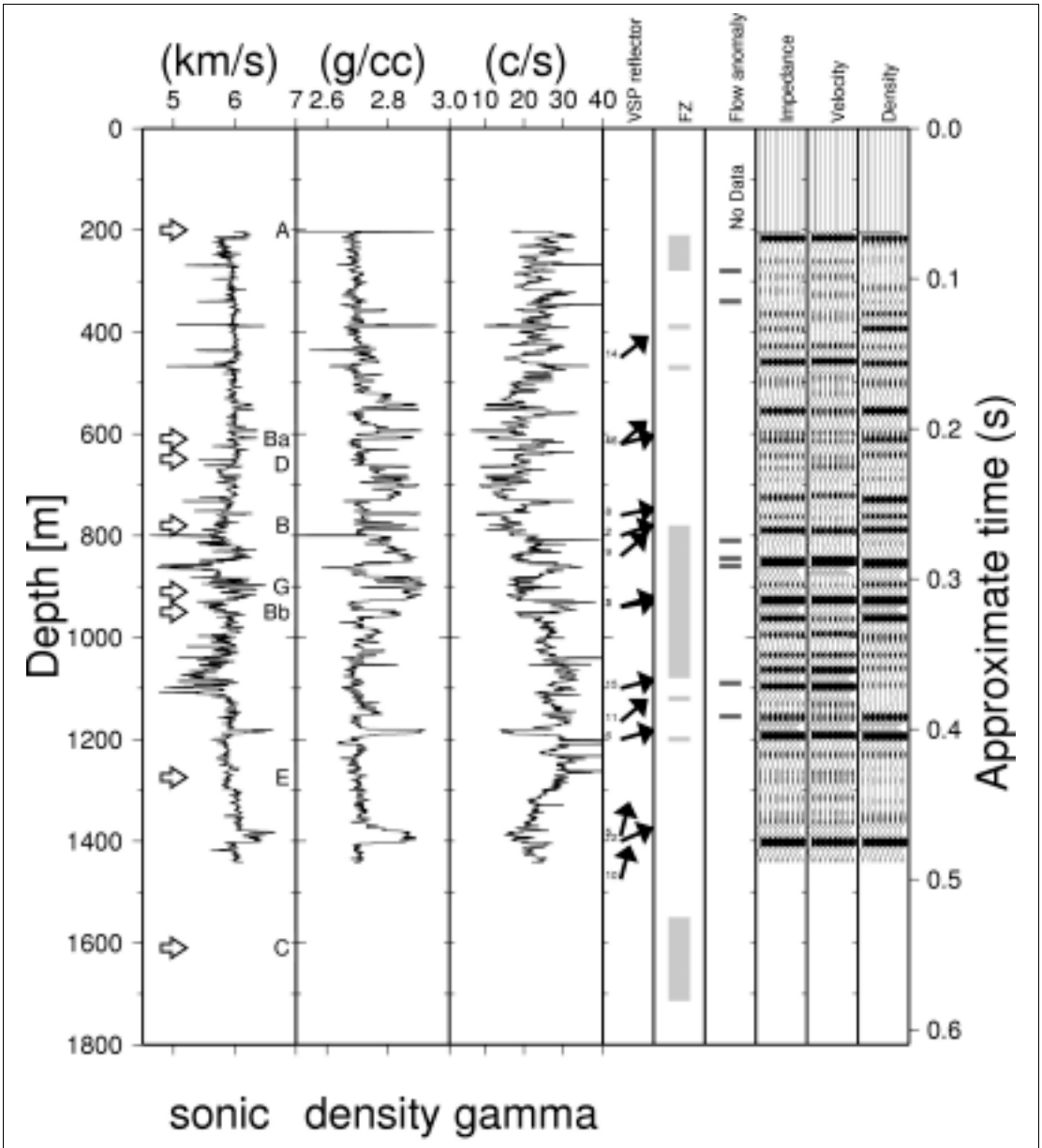

Figure 8−7*. Sonic (SKB log shifted −0.4 km/s), density and gamma logs from the KLX02 borehole. Shown also are zones interpreted to be highly fractured (FZ) in the core and zones where flow anomalies are present. Greenstones stand out as high−density units (density greater than 2.7 g/cc). Log data were not acquired below c. 1430 m, but a major fracture zone is observed in the core in the interval 1550−1714 m. Points where the reflections identified on the surface seismic sections intersect or project into the borehole are marked in the velocity panel. Reflectors identified on the VSP are shown with their corresponding ID number and dip (arrow tail indicates reflector depth). Synthetic seismograms generated using the impedance, only the velocity, and only the density are shown furthest to the right. A Ricker wavelet with a peak frequency of 150 Hz was used for the synthetics and an average velocity of 5850 m/s to calculate the time scale.*

8.4. Modeling of reflections

It is useful to model the reflections that would be observed from a given velocity and density structure. These synthetic seismograms can then be compared to the observed data to determine if the assumed velocity and density structure is consistent with the observations. The modeling algorithm used here is described in Ayraza et al. (2000) and the velocities and densities shown in Table 8−4 have been assumed for the three rock types used. The rock contrasts modeled are granite/fracture zone and granite/greenstone. Although a finite thickness can be given to the reflectors, half spaces are used for simplicity. At this stage it is primarily of interest to match traveltimes and amplitude patterns, not waveforms. Both PP and PS reflections are included when calculating the response.

Table 8−4. Velocities and densities used in the seismic modeling.

Rock type	***Vp (m/s)***	***Vs (m/s)***	**ρ *(kg/m^3)***
Granite	5800	3348	2700
Fracture zone	5000	2700	2500
Greenstone	6800	3400	2900

Figure 8−8 shows the expected VSP response based on the surface seismic model (Table 3−1). A comparison with the observed VSP sections (Figure 7−5) shows that the general pattern of sub−horizontal reflections and moderately dipping reflections is found in the VSP, however, the signature from the steeply dipping events is missing in the synthetic VSP sections. Note also the similar slope of the PS converted wave reflection from the dipping D and G reflectors to that of the PP reflections from the B group. Finally, note that reflections from the A and C reflectors will not intersect the borehole along the synthetic VSP survey.

Figure 8−9 shows the expected VSP response based on the VSP model (Table 8−3). Here, the model response matches the observed data better, as it should since the model is based on the data. Note the difficulty that can be encountered in choosing which reflections are PP and which are PS for the steep events (red reflections in the figure).

Figure 8−10 shows where reflections from the VSP model (Table 8−3) are expected to be observed on the surface seismic data. Interpreted greenstone reflections (blue reflections) fall in the interval with increased sub−horizontal reflectivity on the surface seismic, but generally have higher dips. As mentioned earlier, the VSP reflectors 4 and 9 (black reflections) cannot be correlated to any clear events on the surface seismic although they are sub−parallel to reflection C. The group 3 steep reflectors are also not clearly observed on the surface seismic, although there are some signs of them. If they have been oriented correctly on the VSP, then these would be difficult to distinguish from the sub−horizontal and moderately dipping reflections on Line 1, but should stand out as steeply dipping events on Line 2.

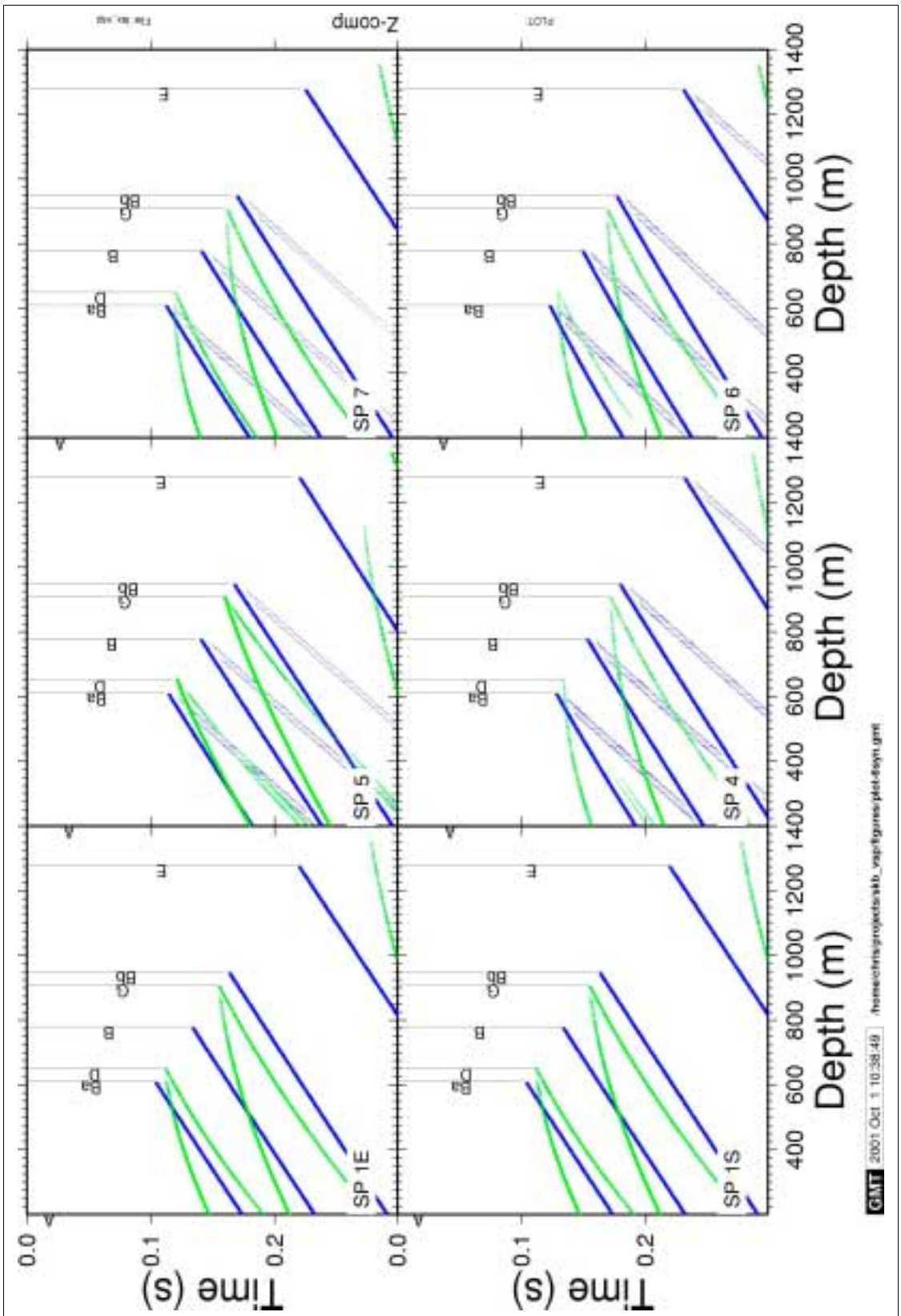

Figure 8−8*. Synthetic vertical component VSP for reflector model given in Table 3−1. Blue reflections are from greenstones and green ones are from fracture zones.*

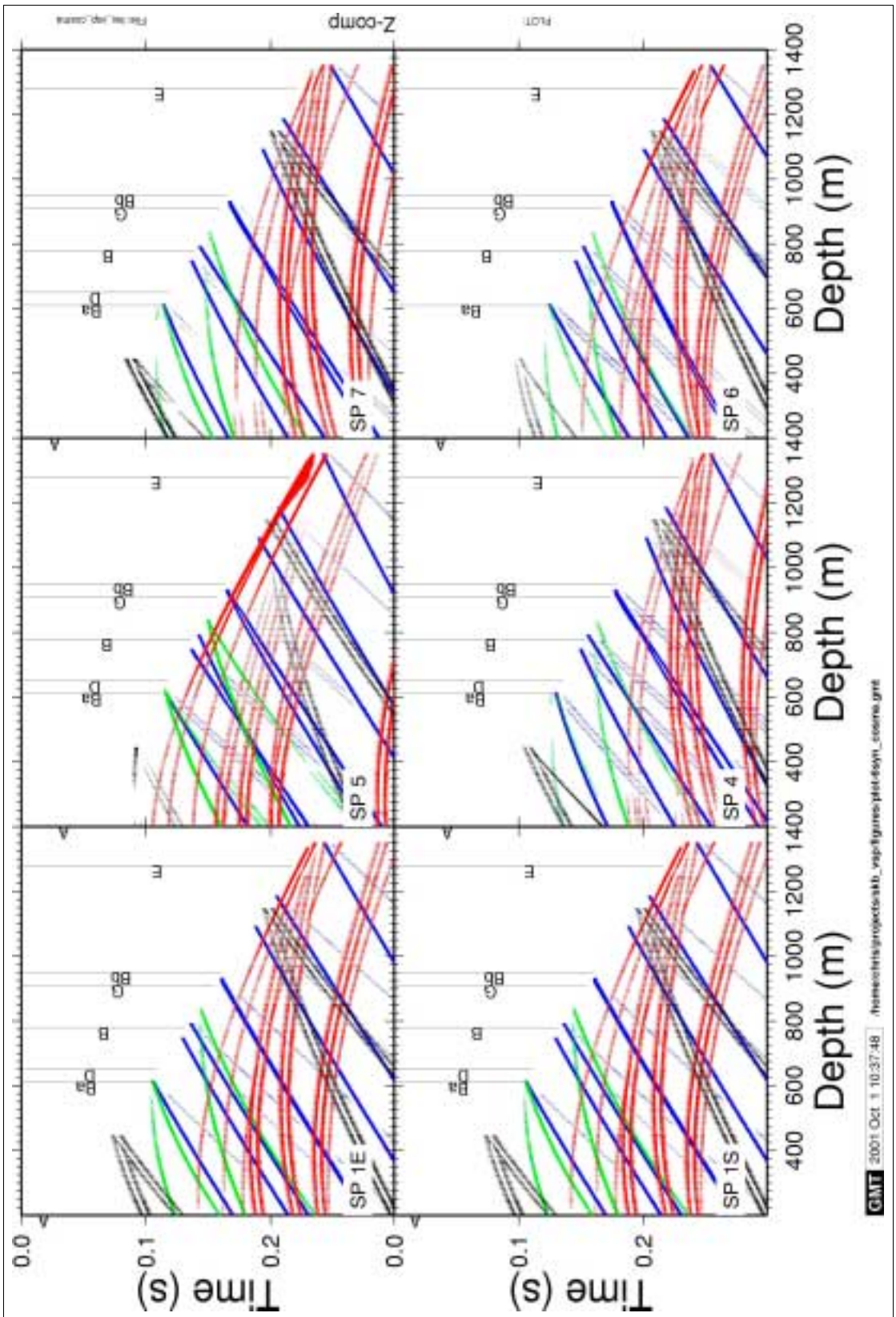

Figure 8−9*. Synthetic vertical component VSP for reflector model given in Table 8−3. Blue reflections are from group1, green ones from group 2a, black ones from group 2b and red ones from group 3.*

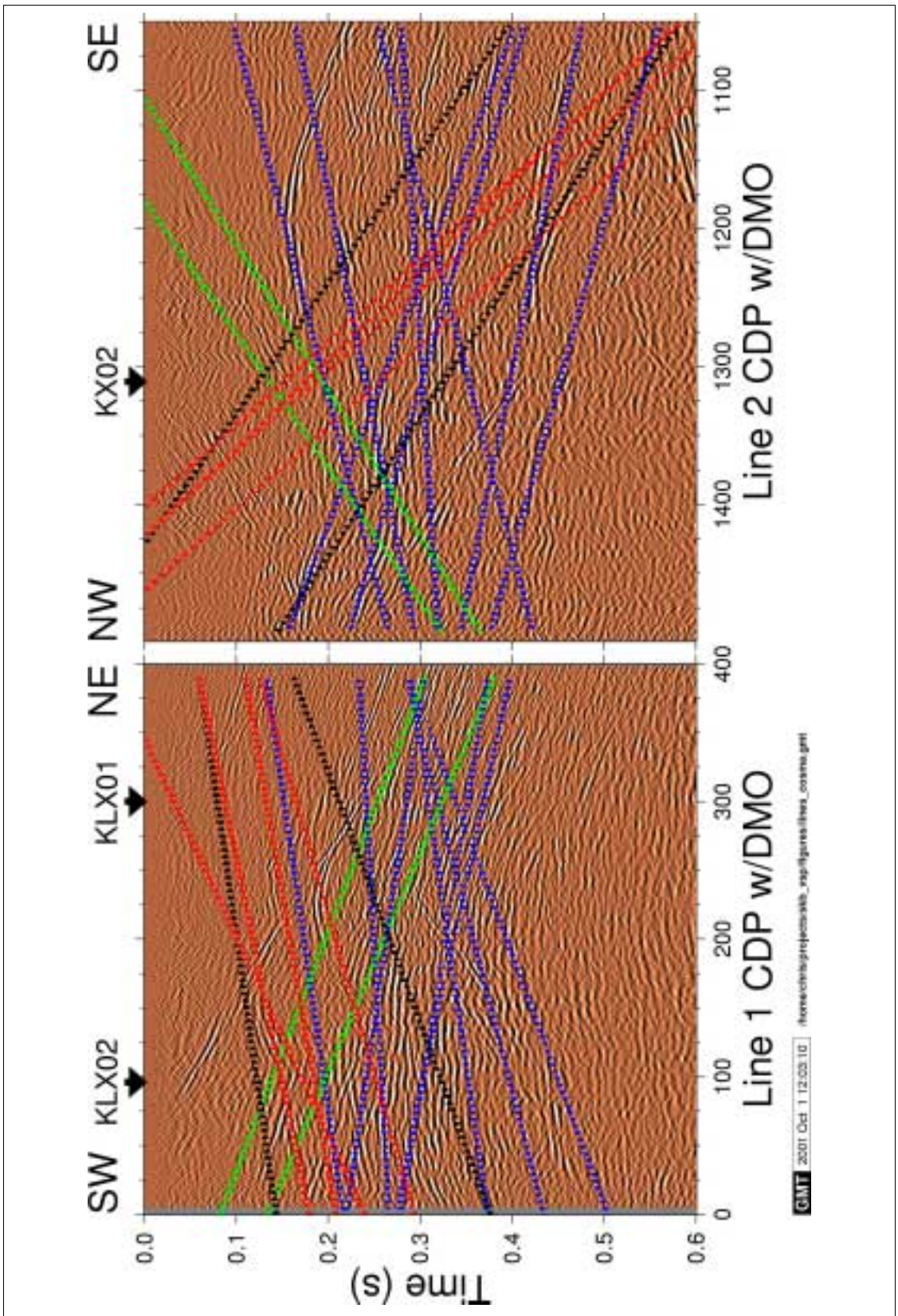

Figure 8−10*. Observed surface seismic sections and synthetic surface seismic based on on VSP results given in Table 8−3. Blue reflections are from group1, green ones from group 2a, black ones from group 2b and red ones from group 3.*

8.5. Casing survey

The most clearly imaged and well oriented reflection on the surface seismic is the A reflection that dips at about 45° and strikes at about 270°. It has been projected to intersect the KLX02 borehole at about 200 m. The main VSP survey ran from 200 m to 1395 m and could, therefore, not image this reflector. For this reason, a special casing survey was run at SP1 with 2.5 m spacing between the geophones to image the A reflector. The data are of somewhat poorer quality in the casing, due to the poorer coupling in the larger diameter (215 mm) section of the borehole. Data processing consisted of simple filtering and removal of the downgoing P−wave and S−wave energy (Figure 8−11). After processing a strong reflection is observed that appears to intersect the borehole between 180 m and 190 m, although it is difficult to trace it all the way to the borehole. The reflection actually appears to consist of two reflections with somewhat different dip. These two reflections can be adequately modeled with the orientation given in Table 3−1 for reflector A as originating from a fracture zone dipping at 43°, striking at 268° and intersecting the borehole at 195 m. The more steeply dipping branch of the reflection is the PP reflection, while the less steeply dipping branch is the PS reflection. It is highly likely that these reflections originate from the same zone as the A reflection on the surface seismic. It is not likely that the casing shoe itself is generating in these events since they would have different traveltimes if this were the case. Note that the PP branch on the VSP cannot be traced all the way to the borehole due to its amplitude variation with angle of incidence. Note also the strong downgoing PS converted wave that is generated at or close to 195 m (Figure 7−3 and Figure 7−4).

Another reflection is also observed on the casing survey that intersects the borehole at about 65 m. This depth is close to the contact between the Äspö diorite and Småland granite at about 68 m suggesting that the reflection may be associated with this boundary.

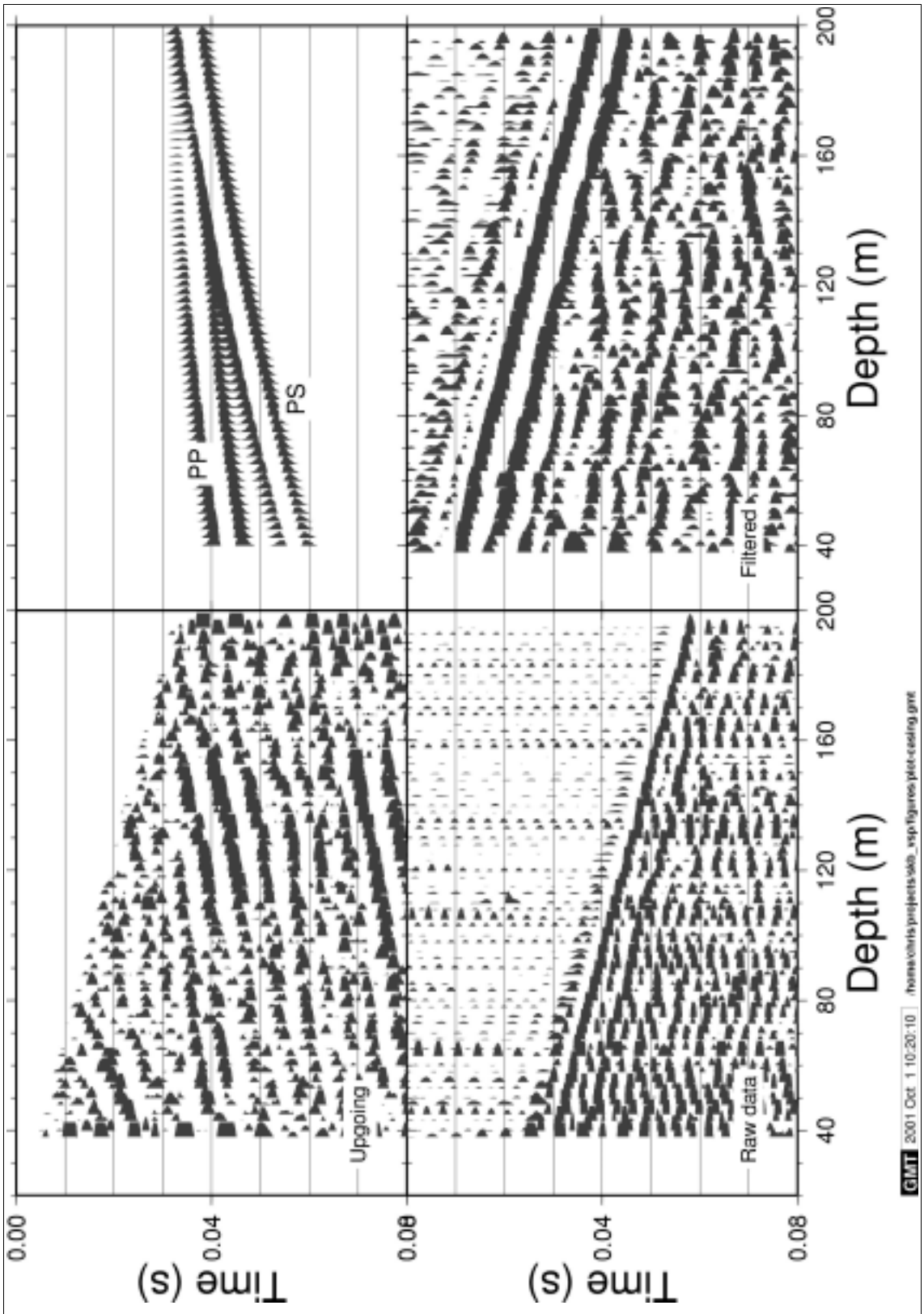

Figure 8−11. *Vertical component data acquired in the casing showing three stages of data processing and modeled data for the A reflector as identified in the surface seismic (Table 3−1).*

8.6. Mederhult zone (Reflector C)

Reflector C on the surface seismic has been interpreted as possibly being connected to the Mederhult zone, a strongly deformed W−E striking zone lying about 1.5 km to the north of KLX02 (SFZ03 in Figure 3−19 in Ekman, 2001). If so, this would be an indication that the zone, or at least a branch of it, dips to the south. The reflection projects into the borehole in the strongly deformed zone at 1550−1700 m, but was not imaged all the way to the borehole on the surface seismic due to the geometry of the experiment. If it continues to the borehole the PP reflection from it would be expected to be observed on the VSP at about 280 ms at depths below 1000 m (Figure 8−8), although its amplitude becomes weak as it approaches the borehole. No such reflection is seen clearly on the VSP. This may be due to:

1. Its amplitude is too weak
2. The zone becomes thin or diffuse over that section which the VSP images it
3. The zone does not extend to the borehole.

Since the VSP did not extend all the way down to its projected intersection with the borehole it is not possible to determine which of the above is the correct answer. A surface seismic profile in the N−S direction over the borehole that continues far enough to the south could answer the question if the zone extends to the borehole.

9. Discussion

9.1. Accuracy of reflector locations

Determining the orientation of reflectors in the rock is of great importance. The accuracy of the orientation is dependent mainly upon four main factors in crystalline rock when using 2D data. Theses are:

1. The accuracy in picking the moveout (changes in arrival dime with distance) of the reflections on the time section.
2. The velocity used to convert from time to depth.
3. The cross−dip component of the reflections.
4. The planarity of the reflections

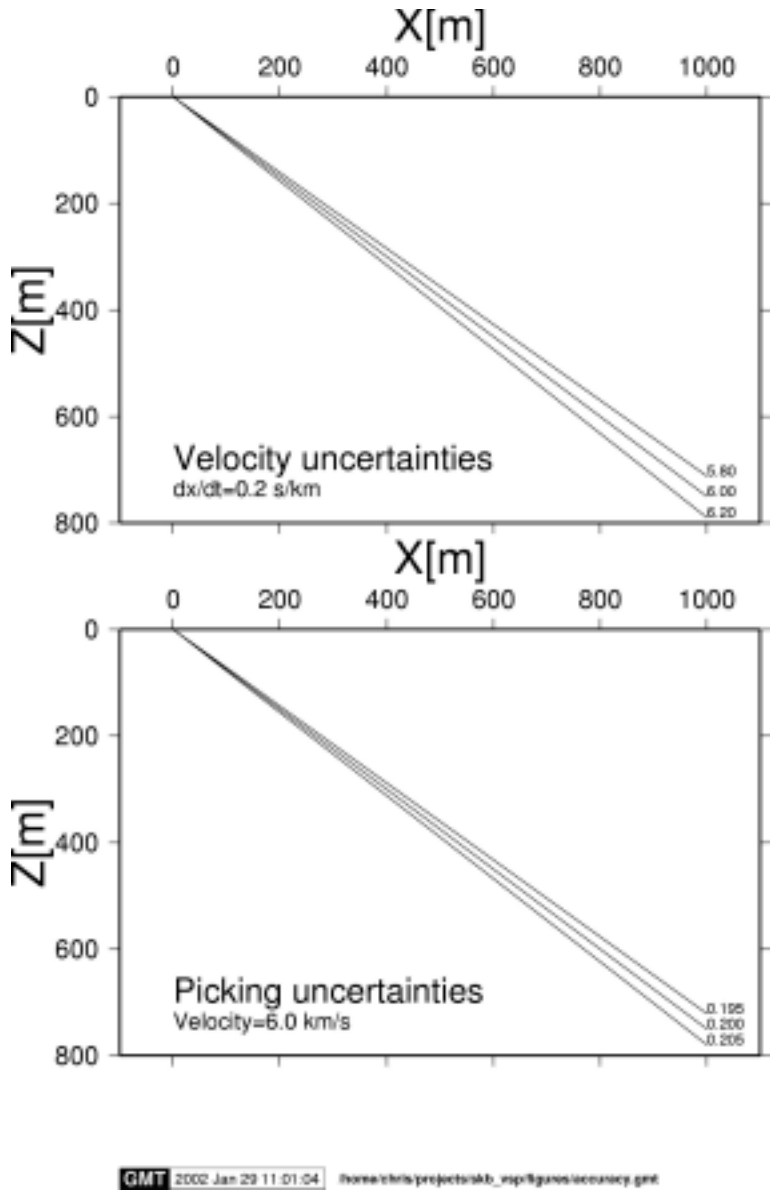

Figure 9−1*. Differences in reflector orientation due to variations in velocity used to convert to depth and in variations in picking the moveout over the time section.*

Moveout of clear reflections can generally be picked to better than 0.005 s/km and velocities are generally known to an accuracy of better than 0.2 km/s. Figure 9−1 shows the differences in reflector orientation due these uncertainties for an interface dipping at about 35° in−the−plane of the profile. At depths of about 750 m the accuracy of the depth determination is about ±40 m or about ±5%. Generally the moveout and velocity are more well determined than this and the accuracy of the depth determination is better than ±5%. A greater uncertainty is due to the strike of the reflection often being unknown. Table 9−1 shows how the estimated dip and depth of a reflector change as the assumed strike of the reflector varies from the true strike. At strike differences greater than about 15° the depth errors exceed those that can be expected from moveout and velocity errors.

The above discussion is based on surface seismic data, but applies equally well to VSP data. In general, the errors in depth estimates will be less in absolute terms on VSP data since the reflectors are closer to the observation points. In the case of the reflector intersecting the borehole, the depth estimate is nearly exact if the intersection point can be picked accurately (difficult for steeply dipping reflections). Errors in dip estimates will generally be of the same order as for surface seismic data, assuming the strike of the reflector is known.

Table 9−1. Estimated dip and depth to a reflector 1000 m away from where the reflector intersects the surface as a function of the difference in the assumed strike to the true strike of the reflector.

Strike difference (degrees)	*Calculated dip (degrees)*	*Calculated depth (m)*
0	35.00	700.21
10	34.39	684.53
20	32.61	639.89
40	26.06	489.13
60	16.67	299.36
80	5.72	100.10
89	0.57	10.01

How planar the reflections are will influence how well their depth can be determined if only 2D data are available. In 3D data the requirement that the reflectors be planes in order to orient them is not necessary. It is probably the lack of planarity of the reflectors that results in the VSP and surface seismic giving different orientations (compare Table 3−1 with Table 8−3). This is due to the reflection points falling along different traces of the reflector where the local orientation may be different from the large scale structure.

9.2. PS conversion problem

The problem of determining whether a reflection is PP or PS does not appear to have been as severe as, perhaps, was expected. Genuine PP reflector seem to have been identified in all cases, except in the data set recorded at shallow depth in the casing (37.5−195 m), from source point SP1. This data set contains a reflector that can be interpreted either as a PP or a PS event and the ambiguity could not be resolved because only one source point was recorded at shallow depths and the discrimination scheme

described earlier could not be applied. Deeper reflectors that could be tested with both PP and PS time functions in all five measured profiles could be interpreted unambiguously as PP reflections.

The consistency from source point to source point does not offer a complete proof of the correctness of the interpretation. Such a proof should be sought by constructing a synthetic model equivalent to the most probable interpretation of the site geological model and test the fitting procedure against it. For an interpretive approach to be correct, it should allow the PP and PS reflectors to be identified, when they are present in the data, but should also state their absence when they are not. In the current interpretation, the PP reflectors were identified in practically all cases, but not so the associated PS conversions. These notable absences are believed to be due to the IP (Image Point) processing sequence, which tends to eliminate all events that cannot be associated with P−wave time functions. It is not yet perfectly clear which PS conversions are suppressed by IP filtering and which go through.

It is therefore suggested that in the future, an equivalent synthetic model is built and run in parallel through a similar processing sequence to the measured data. All processing and interpretive procedures would therefore be tested on this model as a means of quantifying the uncertainty associated with the structural predictions.

9.3. Acquisition considerations

To maintain the costs at a low level, the KLX02 multi−offset VSP was conducted with only five sparse offsets. The estimation of the optimum number of shot points was based on the current experience with explosive sources. However, the practical experience with the SIST1000 demonstrates that the number of shot points could be doubled in the future without a significant increase in the acquisition costs.

For future VSP surveys it would be useful to have twice the number of shot points (on the order of 10) and two tractors operating in parallel in order to increase the capability to correlate reflections from shot point to shot point. The cost increase with the SIST1000 source would be comparatively small for such an operation.

Given the sparse shot distribution used at KLX02, two assumptions have been made: that the fracture zones follow planar trends and that the same reflectors can be identified in the profiles measured from several shot−points.

The planarity assumption has typically to be valid over a reflector with an extension of the order of half the distance between adjacent shot−points, i.e. approximately 200−300 m in the KLX02 case, and intersecting at a depth of the same order or larger. The planarity assumption has been verified with all of the multi−offset VSP investigations conducted in crystalline rock. Conversely, if the shot points are too sparse or the target reflector is shallow, situations may appear in which the interpretation based on consistency of orientation in several profiles may be erroneous. Therefore, a denser shot grid, or clusters of shot arrays are a welcome extension whenever possible.

The parallel model suggested above as a means of increasing the confidence in the result of the VSP surveys could in fact also be very valuable for evaluating the most adequate shot distribution and density for a typical case based on the Laxemar KLX02 survey. In addition, a source array should be considered when acquiring data. Such an array would consist of a 7 station by 7 station cross with the source points spaced at 3−5 m within the cross. By acquiring data with a source array it should be possible to better separate the wave field into its different components and identify exactly where reflections intersect the borehole. The added cost of having a 15 station array compared

to a single station at every source point is significant, but not immense. Much of the cost of the SIST1000 source is the driving time between the different source points. At present, the preferred scenario would involve clusters of shots disposed as cross−shaped arrays with transverse directions of the order of one wavelength, i.e. c. 30 m, at 5 m intervals. These arrays would have a stronger directional filtering effect on steeply inclined reflectors than on the sub−horizontal ones, as the wavefront reflected on the latter would be nearly synchronous for all the shots in the array. This is exactly where the added information would mostly be needed, as sub−horizontal reflectors are normally detected in both surface seismic and VSP profiles and, therefore, the need for independent validation is less acute.

10. Conclusions and recommendations

After tuning the processing sequence for the SIST1000 source, high quality seismic sections were obtained from the 5 shot points where the source was used over the entire survey section. The project shows that the SIST1000 source is well suited for VSP studies down to 1500 m in crystalline rock. The energy put into the ground by the SIST1000 source is greater than the explosive 15 gram slim−hole source recommended for surface seismic surveying, but the frequency content is lower.

Analyses of the amplitude decay with shows that the rock in the Laxemar area has a Q (seismic attenuation) value between 50 and 100, a typical value for the uppermost km in the Baltic Shield.

The VSP in KLX02 confirms the surface seismic interpretation of a complex structure where fracture zones and lithological boundaries produce reflections. There is general agreement between where reflections are observed on the surface seismic and where they are located in the borehole, although there is not a one to one correspondence. Discrepancies can be attributed to the VSP images the local structure around the borehole while the surface seismic is more sensitive to the larger scale regional structure.

Three sets of reflections are observed on the VSP. These are:

- Group 1: Sub−horizontal to gently dipping reflectors with varying dip that probably correspond to the interpreted greenstone reflections on the surface seismic.
- Group 2: Moderately dipping reflectors with two sub−groups, one with NNW dips and the other with SSE dips. The former corresponds to reflections B and G on the surface seismic, while the latter is not observed.
- Group 3: Steeply SE dipping reflectors with strikes of 50−70°. These are not directly observed on the surface seismic, but may be correlated to the regional fracture zone SFZ04 (Ekman, 2001).

Since the VSP and surface seismic data give information on different scales, caution should be used when extrapolating VSP reflectors to the surface. This is especially gently dipping ones, since they are imaged over fairly small areas and it is difficult to determine their true strike and dip.

For future VSP surveys it would be useful to have twice the number of shot points (on the order of 10) and two tractors operating in parallel in order to increase the capability to correlate reflections from shot point to shot point. The cost increase with the SIST1000 source would be comparatively small for such an operation.

In addition, a source array should be considered when acquiring data. Such an array would consist of a 7 station by 7 station cross with the source points spaced at 3−5 m within the cross. By acquiring data with a source array it should be possible to better separate the wave field into its different components and identify exactly where reflections intersect the borehole. The added cost of having a 15 station array compared to a single station at every source point is significant, but not immense. Much of the cost of the SIST1000 source is the driving time between the different source points.

11. Suggested future work

Aside from more work being required on the preprocessing side in order to determine the optimum parameters for generating the ”raw” sections there are, at present, three problems which need addressing. These are

- Discrimination between PP and PS reflections

  In order to orient the interfaces that produce the observed reflections it is important to know if the reflection being analyzed is a PP or PS reflection. The IP transform appears to favor passing only PP reflections and the consistency of the source point to source point analyses indicates all interpreted reflections in the main VSP survey are PP reflections. However, there is still significant uncertainty, especially for the steeper events. By processing synthetic data containing both PP and PS reflections from geological models (such as the RVS model) then an assessment can be made as to how well PS reflections are suppressed in the processing and interpretation flow.

- Testing of source arrays compared to single sources at the source point

  In areas with complex structure, such as Laxemar, the recorded seismograms consist of overlapping reflections originating from interfaces with various orientations. Often it is the response from lithological contrasts which dominate the sections, rather than the fracture zones. By acquiring data using source arrays rather than single source points, wavefronts may be synthesized that are sensitive only to interfaces with a certain orientation. The feasibility of using such arrays can be tested in the computer using realistic geological models. The increase in field acquisition time using source arrays rather source points is envisioned to double. However, if the imaging of steeply dipping structures and their projected intersections with the borehole can be improved then this increase is well justified.

- Discrepancy between observed dips on the VSP compared to the surface seismic

  The general structural trends are consistent between the VSP and surface seismics, however, the VSP tends to show consistently steeper dips. Strong support for the VSP results is found in the borehole logs and that strong support for the surface seismic results is found in practically all geological appraisals related to the site. The current hypothesis is that the seemingly poor match is in fact the result of the difference of scale of the two surveys. The VSP surveys are more local in nature but sense a wider aperture of dips and should therefore be compared only against the corresponding parts of the surface profiles. The interpretation performed along these lines is bound not only to reduce or eliminate inconsistencies, but also to increase the understanding of the geological structure.

All of the above problems can be studied using synthetic or existing data. No new acquisition is necessary at this point.

References

Ayarza, P., Juhlin, C., Brown, D., Beckholmen, M.,Kimbell, G., Pechning, R., Pevzner, L., Pevzner, R., Ayala, C., Bliznetsov, M., Glushkov, A. and Rybalka, A., 2000. Integrated geological and geophysical studies in the SG4 borehole area, Tagil Volcanic Arc, Middle Urals: Location of seismic reflectors and source of the reflectivity, J. Geophys. Res.: 105, 21333−21352.

Bergman, B. Juhlin, C. and Palm, H., 2001. Reflexionsseismiska studier inom Laxemarområdet, SKB, R−01−07.

Cosma C., Juhlin C. and Olsson O., 1994. Reassessment of seismic reflection data from the Finnsjön study site and prospectives for future surveys, SKB, TR−94−03.

Cosma, C. and Heikkinen, P., 1996. Seismic investigations for the final disposal of spent nuclear fuel in Finland. Journal of Applied Geophysics: 35, 151−157.

Ekman, L., 2001. Project Deep Drilling KLX02 − Phase 2: Methods, scope of activities and results − Summary report, SKB, TR−0−11.

Gorbatschev, R. and Bogdanova, S., 1993. Frontiers in the Baltic Shield. Precambrian. Research: 64, 3−21.

Hardage R, 2000. Vertical Seismic Profiling, Principles. Handbook of Seismic Exploration: Seismic Exploration, v.14 Pergamon Press, 570 pp.

Juhlin, C., 1995. Imaging of fracture zones in the Finnsjön area, central Sweden, using the seismic reflection method. Geophysics: 60, 66−75.

Juhlin C. and Palm H., 1999. 3D structure below Ävrö island from high resolution reflection seismic studies, southeastern Sweden. Geophysics: 64, 662−667.

Juhlin, C., Palm, H. and Bergman, B., 2001. Reflection seismic imaging of the upper crystalline crust for characterization of potential repository sites: Fine tuning the seismic source, SKB, TR−01−31.

Milnes, A. G, Gee, D. G. and Lund, C.−E., 1999. Crustal structure and regional tectonics of SE Sweden and the Baltic Sea, SKB, TR−95−36.

Park, C. B., Miller, R. D., Steeples, D. W. and Black, R. A., 1996. Swept impact seismic technique (SIST): Geophysics: 61, 1789−1803.

Talbot, C. J., 1990. Some clarification of the tectonics of Äspö and its surroundings. SKB, PR 25−90−15.

Weihed, P., Bergman, J., & Bergström, U., 1992. Metallogeny and tectonic evolution of the early Proterozoic Skellefte district, northern Sweden. Precambrian Research: 58, 143−167.

Appendix A−1. Wireline logging

GEOPHYSICAL LOGGING IN BOREHOLE LAXEMAR KLX02

1. Surveys Performed

- Resistivity
- Natural Gamma
- Full Waveform Sonic

2. Equipment specifications

Equipment provider :	Mount Sopris Instrument Co.
Probes :	2PIA−1000 Conductivity−Induction, 2PGA−1000 Natural Gamma, 2SAA−1000 Full Wave Form Sonic
Accessories :	1000m of 1/8 in cable, Electrical winch, Data logger, field Computer
2SAA−1000 Sonic probe specifications	
Operating temperature range :	−20 to 70 degrees C
Maximum pressure :	3000 PSI
Sample resolution :	12 bits
Length :	205.42 m
Diameter :	0.04445 m
Weight :	9.7 Kg
Isolator length (Between TX and Rx1):	0.914 m
Sonic probe configuration	
Number of transmitters :	1
Number of receivers :	2
Type of receivers :	Piezoelectric
Transmitter−receivers spacing :	Tx−Rx1 : 0.914 m; Tx−Rx2 : 1.219 m
Sonic log operating features	
Transmitter frequencies :	20 kHz down hole; 30 kHz up hole
Operating logging speed :	2.5 m/min down hole; 3.5m/min up hole
Sampling in depth :	0.05 m
Holdoff time :	50 micro−seconds
Sample rate :	4 micro−seconds
Number of samples :	512
Total sampling time length :	2048 micro−seconds
Receiver gain :	Automatic
Operating mode :	Monopole
Number stacked :	1

3. Preparation−Calibration

0* No calibration was performed for the Natural−Gamma probe.
1* Surface calibration was done with the induction tool in coil. (100 micro−siemens driver with 0 micro−siemens and 91 micro−siemens calibration)
2* Gamma and induction probes were assembled to use both logs in the same run.

Selecting the Cutoff frequency for the Full Waveform Sonic logging

A first run was attempted with the probe set at a center frequency of 10 kHz. Severe tubewave saturation was noticed.

The recommended cutoff frequencies for the 2SAA−1000 sonic−probe are:

$$f_{pco} = \frac{v_p}{2.5 \cdot D} \qquad f_{sco} = \frac{v_s}{1.2 \cdot D}$$

Where:
f_{pco} = compression wave cutoff frequency
f_{sco} = shear wave cutoff frequency
Vp and Vs = expected compression and shear rock velocities (5800 m/s and 3400 m/s)
D = borehole diameter (0.076 m)

The recommended cutoff frequencies for the compression and shear mode are are:

f_{pco} = 30 526 Hz
f_{sco} = 37 280 Hz

Therefore, a 30 kHz (±50%) transmitter center frequency was chosen. However, an additional run was performed with the transmitter set at 20 kHz (±50%), as an attempt to lower the frequency within the range allowed by the borehole diameter.

4. Full Sonic Wave Processing

The processing was done by the WellCAD software from ALT. Both raw and band−pass filtered data sets were used for the determination of the velocities. The semblance analysis involving data recorded with both receivers appeared to be more effective when applied to the raw records. The analysis was performed on the 30 kHz data, as the frequency band (15 kHz to 45 kHz) includes the cutoff frequencies for both the compression and the shear waves.

The tubewave analysis did not lead to the identification of clear secondary (reflected) tubewaves, the low velocity tubewaves being spatially aliased at the relatively high frequencies used to emphasize the response of the compression and shear waves. The integrated tubewave energy was computed and shows a stable behavior. The window parameters for tubewave analysis were:
Offset: 760 us
Blanking: 1000 us
TX frequency: 30 kHz
Fluid Velocity: 666 us/m

Both sides of the windows were considered.

The Poisson's coefficient used VAM_Vp and VAM_Vs log.

5. Presentation of the Results

The result of the velocity analysis is presented in the attached document.
The following parameters are represented (Left to right):

1 Natural gamma log in cps;
2 Resistivity log in ohm.m;
3 Depth in meters;
4 Full waveform of the first receiver in microseconds;
5 Tube wave energy integrated in the specific windows defined in the WellCAD process;
6 Velocity analyzed by semblance process in microseconds per meter;
7 VAM_Vp, Velocity analyze adjusted to the maximum for the compression velocity;
8 VAM_Vs, Velocity analyze adjusted to the maximum for the shear velocity;
9 Poisson's Ratio.

6. Conclusions

The semblance analysis permits the evaluation of both the compression and shear velocities. The mean compression velocity is approximately 5880 m/s and the mean shear velocity is around 3440 m/s, which is close to the values expected. The Poisson's ratio is between 0.2 and 0.3. Problems with the computation of the Poisson's ratio appear in fracture zones, where picking errors may result in non−physical values for Vp and Vs.
The fracture identification is based on all curves and full waveform observations: Tube waves attenuation, Poisson's Ratio "jump", Vp and Vs curves.

Appendix A−2. Coordinates of all VSP source points

The following records were made with the same receiver chain orientation:

1_explo, 1_sist1000, 1_sist50, 2_sist1000 and 7_sist1000 (7_sist1000 depths 360−1355 m)

4_sist1000, 5_sist1000, 6_sist1000 and 7_sist1000 (7_sist1000 depths 200−355 m)

Receiver depths for each source position:

Source	Depths (m) and remarks	Receiver spacing (m)
SP1 explosives	200−1355	5.0
SP1 SIST1000	200−1355	5.0
SP1 SIST1000	37.5−195.0	2.5
SP1 Sist50	200−275,320−515,560−595, 680−715,840−875	5.0
SP2 explosives	200−235,320−355,440−475, 560−595,680−715,800−835, 920−955, 1040−1075,1160−1195,1280−1315	5.0
SP2 SIST1000	200−235,320−355, 440−475,560−595, 680−715, 800−835, 920−955, 1040−1075,1160−1195,1280−1315	5.0
SP4 SIST1000	200−1355	5.0
SP5 SIST1000	200−1355	5.0
SP6 SIST1000	200−1355	5.0
SP7 SIST1000	200−1355 (640−675 data missing)	5.0

KLX02 borehole coordinates used (RT90 and RH70):

	North	East	Elevation
KLX02:	6366768.597	1549224.233	18.31

Shot positions were (RT90 and RH70):

Code	North	East	Elevation	Source
1	6366778.10	1549208.34	16.44	SIST1000 and Sist50, Source position 1a
111	6366780.27	1549214.62	16.38	SIST1000 and Sist50, Source position 1b
11	6366779.04	1549207.8	16.43	Explosives, Source position 1
12	6366779.77	1549208.43	16.32	Explosives, Source position 1
13	6366778.71	1549206.83	16.29	Explosives, Source position 1
14	6366778.20	1549205.95	16.33	Explosives, Source position 1
15	6366777.30	1549206.49	16.19	Explosives, Source position 1
16	6366776.53	1549207.23	16.08	Explosives, Source position 1
17	6366775.79	1549207.85	15.99	Explosives, Source position 1
18	6366776.44	1549208.97	16.13	Explosives, Source position 1
19	6366777.13	1549210.04	16.45	Explosives, Source position 1
101	6366778.00	1549209.52	16.41	Explosives, Source position 1
102	6366778.82	1549208.90	16.41	Explosives, Source position 1
2	6366661.02	1549135.34	8.46	SIST1000, Source position 2
21	6366657.51	1549131.42	8.43	Explosives, Source position 2
22	6366656.04	1549131.81	8.36	Explosives, Source position 2
23	6366654.58	1549132.38	8.38	Explosives, Source position 2
24	6366653.29	1549133.05	8.28	Explosives, Source position 2
25	6366653.83	1549134.38	8.28	Explosives, Source position 2
26	6366654.41	1549135.83	8.26	Explosives, Source position 2
27	6366654.95	1549137.25	8.24	Explosives, Source position 2
28	6366656.24	1549136.46	8.34	Explosives, Source position 2
29	6366657.48	1549135.69	8.42	Explosives, Source position 2
201	6366658.68	1549134.76	8.47	Explosives, Source position 2
202	6366658.07	1549133.04	8.48	Explosives, Source position 2
4	6366797.36	1549664.60	14.75	SIST1000, Source position 4
5	6367123.74	1549203.58	9.90	SIST1000, Source position 5
6	6366596.20	1548905.59	11.79	SIST1000, Source position 6
7	6366684.25	1549428.35	17.44	SIST1000, Source position 7

Appendix A−3. The SIST Concept − Decoding of the VIBSIST Signals

The principle of the VIBSIST sources explained through the following synthetic example.

Figure A3−1 depicts a 20−level portion of a synthetic VSP profile. The data contains the down−going direct wave field and three up−going reflection events. The shape of the source wavelet, the position and the relative amplitude of the reflection events have been modeled after a real VSP survey conducted with explosives. Unlike the real records, the synthetic traces contain only the four elements mentioned above (direct wave and three reflections) but no background noise, scattering or converted wave modes of any kind.

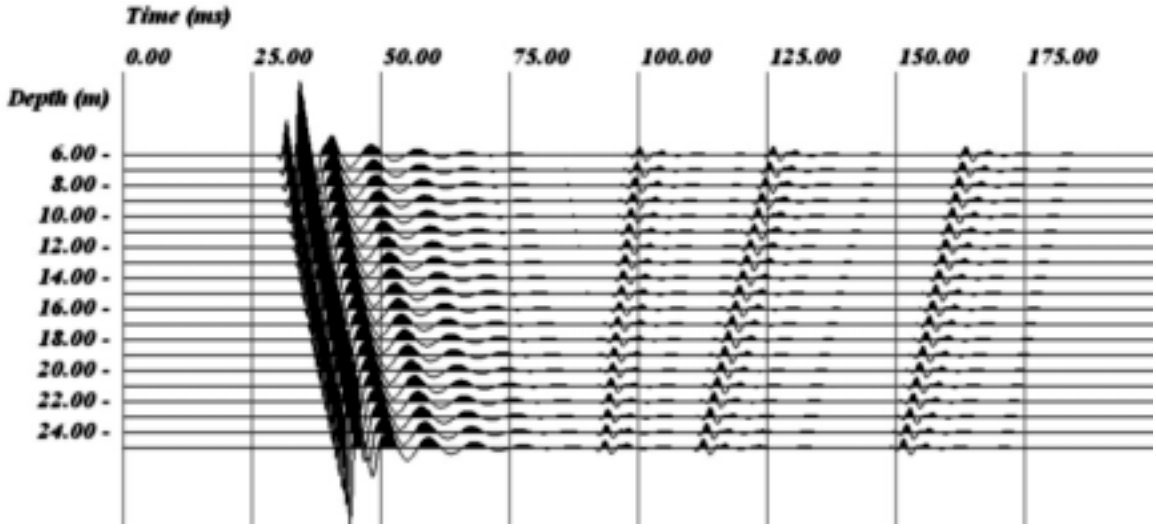

Figure A3−1*. Example of a synthetic VSP profile, down−going and up−going wavefields.*

The time series in *Figure A3−1* can be written symbolically as:

$s_1(t) = s(t) * e(t)$

where, $s(t)$ is the source signature, $e(t)$ is the earth impulse response, and * is the convolution operator.

A similar set of records obtained by a VIBSIST source would look like that shown in *Figure A3−2*.

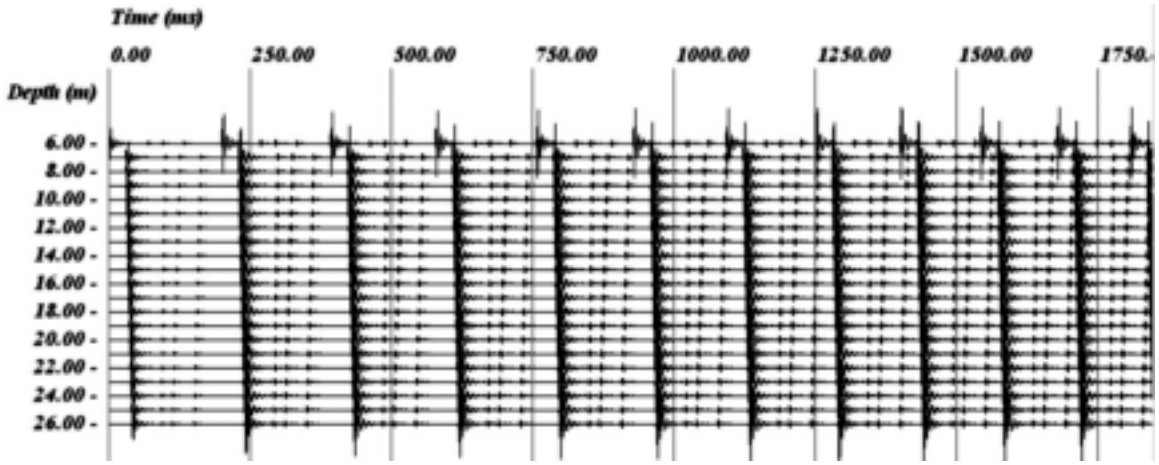

Figure A3−2*. Long synthetic VIBSIST record.*

Compared with *Figure A3−1*, the VIBSIST records in *Figure A3−2* are longer (to depict this feature the horizontal axis has been compressed). The VIBSIST records consist of a large number (normally 100 to 1000) of impacts produced at monotonously varying time intervals. This can be written as:

$s_2(t) = \psi(t) * s_1(t)$

where $\psi(t)$ is the VIBSIST time impact sequence.

Unlike with synthetics, in the real case, the noise cannot be neglected. Therefore, the data from *Figure A3−2* would look more like that shown in *Figure A3−3*.

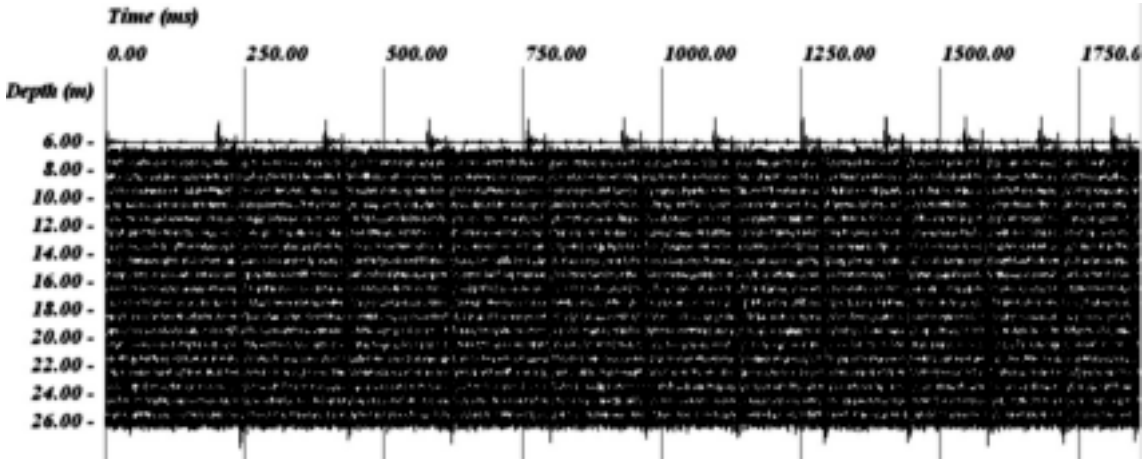

Figure A3−3*. Long synthetic real−life like VIBSIST record.*

$r_c(t) = s_2(t) + n(t)$

where $n(t)$ is the added wide−band noise.

The key idea of the SIST concept is to compute the time function

$r_d(t) = \psi(t) \otimes r_c(t) = ACF\{\psi(t)\} * s_1(t) + \psi(t) * n(t)$

where *ACF* is the autocorrelation operator.

One should note in the expression above that the second term $\psi(t)*n(t)$ tends to zero, as random noise tends to get cancelled through correlation. It follows that:

if $ACF(t) = 1$ at $t = 0$ and $ACF(t) = 0$ elsewhere,

then $r_d(t) = s_1(t)$

In other words, the VIBSIST and the single−pulse signals will become similar, with the benefit on the VIBSIST of allowing noise canceling.

The result of the operation described above is shown in *Figure A3−4*, which is indeed very close to the noise−free synthetic profile of *Figure A3−1*.

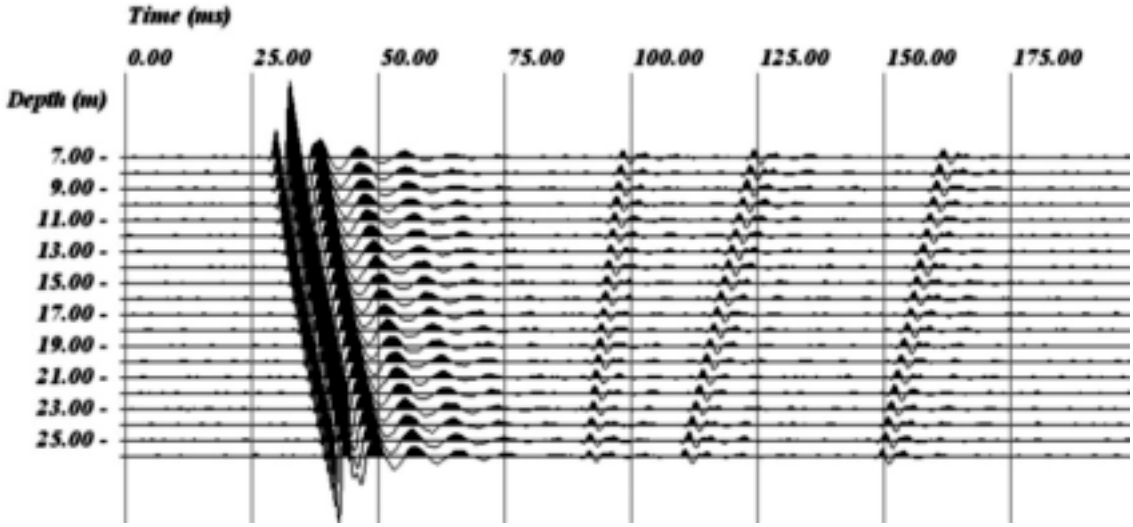

Figure A3−4*. Decoded VIBSIST record.*